Journal of Medicinal Chemistry

Article

Ugi reaction-derived #-acyl aminocarboxamides bind to phosphatidylinositol 3-kinase-related kinases, inhibit HSF1-dependent heat shock response, and induce apoptosis in multiple myeloma cells

Matthias Bach, Anna Lehmann, Daniela Brünnert, Jens T. Vanselow, Andreas Hartung, Ralf C. Bargou, Ulrike Holzgrabe, Andreas Schlosser, and Manik Chatterjee

J. Med. Chem., **Just Accepted Manuscript** • Publication Date (Web): 28 Apr 2017

Ugi reaction-derived α–acyl aminocarboxamides bind to phosphatidylinositol 3-kinase-related kinases, inhibit HSF1-dependent heat shock response, and induce apoptosis in multiple myeloma cells

Matthias Bach[4, ¥], Anna Lehmann[1, ¥], Daniela Brünnert[2, ¥], Jens T. Vanselow[4], Andreas Hartung[1], Ralf C. Bargou[3], Ulrike Holzgrabe[1*], Andreas Schlosser[4, §], Manik Chatterjee[2, §].

[1] Institute of Pharmacy and Food Chemistry, University of Würzburg, Am Hubland, 97074 Würzburg, Germany

[2] Department of Internal Medicine II, Translational Oncology, University Hospital of Würzburg, Versbacher Str. 5, 97078 Würzburg, Germany.

[3] Comprehensive Cancer Center Mainfranken, University Hospital of Würzburg, Versbacher Str. 5, 97080 Würzburg, Germany.

[4] Rudolf Virchow Center for Experimental Biomedicine, University of Würzburg, Josef-Schneider-Str. 2, 97080 Würzburg, Germany.

*Corresponding author: *ulrike.holzgrabe@uni-wuerzburg.de* (Ulrike Holzgrabe)

Tel.: +49-931 31-85460; Fax: +49-931 31-85494.

[¥] These authors contributed equally

[§] Both authors contributed equally

Abstract

The heat shock transcription factor 1 (HSF1) has been identified as a therapeutic target for pharmacological treatment of multiple myeloma (MM) However, direct therapeutic targeting of HSF1 function seems to be difficult due to the shortage of clinically suitable pharmacological inhibitors. We utilized the Ugi multicomponent reaction to create a small, but smart library of α-acyl aminocarboxamides, and evaluated their ability to suppress heat shock response (HSR) in MM cells. Using the INA-6 cell line as MM model, and the strictly HSF1-dependent HSP72 induction as a HSR model, we identified potential HSF1 inhibitors. Mass spectrometry-based affinity capture experiments with biotin-linked derivatives revealed a number of target proteins and complexes, which exhibit an armadillo domain. Also, four members of the tumor-promoting and HSF1-associated phosphatidylinositol 3-kinase-related kinase (PIKK) family were identified. The antitumor activity was evaluated, showing that treatment with the anti-HSF1 compounds strongly induced apoptotic cell death in MM cells.

Keywords

Multiple myeloma, HSF1, Ugi reaction, PIKKs, DNA-PK, affinity capture, quantitative mass spectrometry, armadillo domain

Introduction

The evolutionarily highly conserved heat shock response (HSR) buffers fatal proteotoxic effects in acutely stressed cells and thus prevents induction of cell death.[1] As a central HSR regulator, the heat shock transcription factor 1 (HSF1) controls expression of multiple heat shock proteins (HSPs) which are essential for cellular growth at physiologically relevant conditions by supporting correct protein folding and protein translocation.[2] Previous investigations demonstrated that the HSF1/HSP transcriptome is critically involved in malignant transformation, inhibition of stress-mediated programmed cell death (apoptosis) and malignant growth of human cancer.[3-4] These findings might explain the observed correlation between increased HSP expression and resistance to chemotherapeutic treatment.[5-6] HSF1 as well as HSPs like HSP90 or HSP70 have therefore been intensely studied as potential anti-cancer targets.[3,7-8]

Multiple myeloma (MM) remains a largely incurable B cell neoplasm mainly due to the development of resistance against initially effective therapeutic agents.[9-10] Increasing experimental and clinical evidence suggests that vulnerability of MM cells to proteotoxic stress represents a therapeutic target, as evidenced by the successful clinical establishment of pharmacological proteasome inhibition. Accordingly, HSPs have been shown to critically contribute to the malignant phenotype of MM.[11-15] In addition, we could recently demonstrate a key role of HSF1-dependent HSP induction in response to treatment of MM cells with proteasome or HSP90 inhibitors.[16] This finding indicates that the development of combination approaches including HSF1 inhibition might represent a promising therapeutic strategy overcoming HSR-mediated drug resistance in MM. However, the shortage of clinically suitable pharmacological HSF1 inhibitors currently impairs further clinical

translation.

Previously, a number of structurally diverse compounds were found to putatively inhibit the HSF1-regulated heat shock response.[17-18] The Workman group identified a 4,6-substituted pyrimidine (**1**)[19] as well as the bisamide CCT251236 (**2**)[20] (Figure 1) as strong inhibitors of HSF-1 stress pathway. Those compounds have the chance to be tested in preclinical and clinical trials. The chemical scaffold for a variety of natural compounds ranges from the flavonoid quercetin (**3**)[21] to the benzylidene lactame KNK437 (**4**),[22] natural products like stresgenin B (**5**)[23] produced by a *Streptomyces* sp. AS-9 strain and triptolide (**6**)[24] isolated from *Tripterygium wilfordii* (Figure 1). A recent screening of over 80,000 natural and synthetic compounds, evaluated by Santagata and colleagues,[25] revealed that diverse chemical classes of natural products were successfully tested for their anticancer activity by targeting the HSF1-dependent stress response. Analysing the structural similarities between the compounds dehydrocurvularin (**7**),[25] withaferin A (**8**),[25] colletofragarone A2 (**9**)[25] and the previous mentioned **3-6**, it becomes apparent that all these substances share an α,β-unsaturated carbonyl moiety (Figure 1).

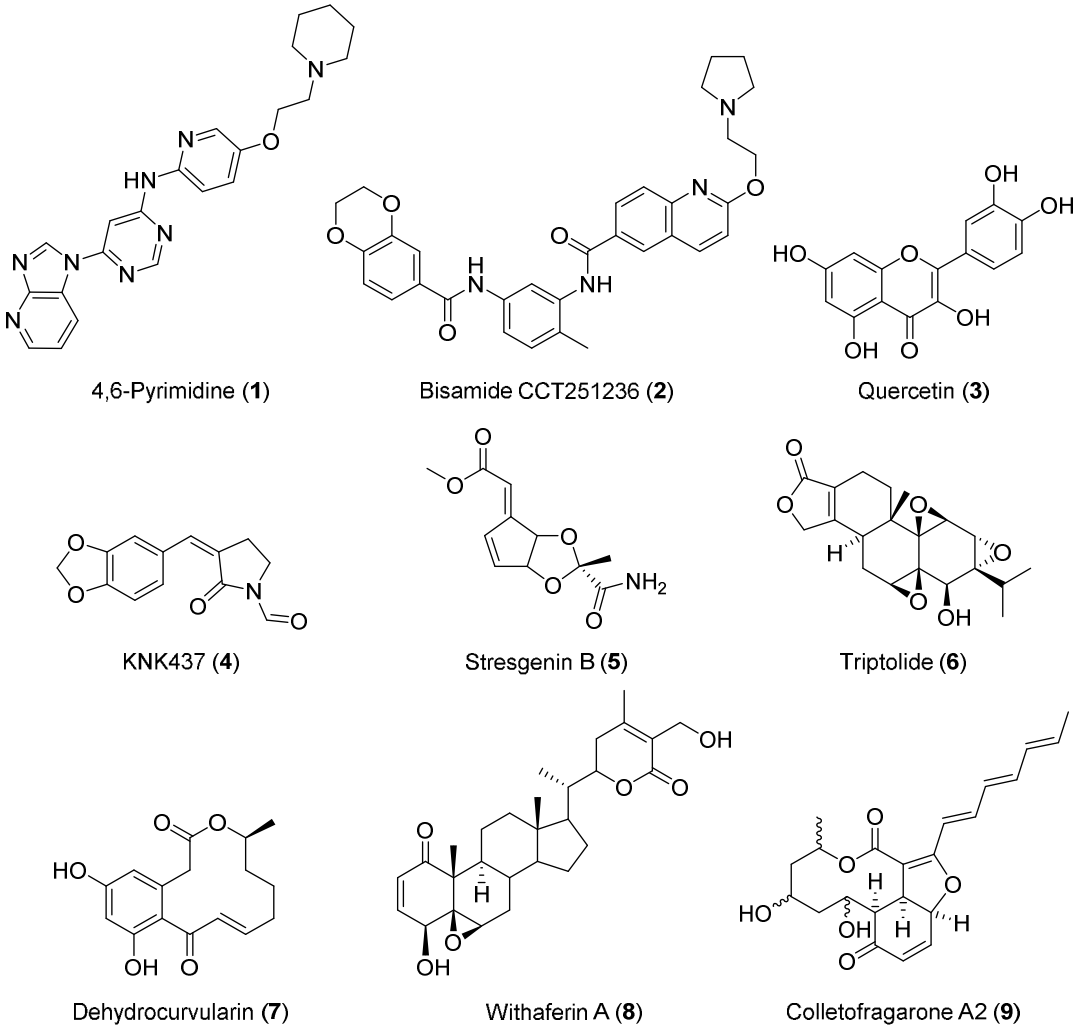

Figure 1: The identified compounds **1**–**9**[19-25] block the HSF1-regulated heat shock response.

Here, we aimed to investigate the importance of this α,β-unsaturated carbonyl moiety for HSF1-related activity (structure-activity relationship) and synthesized a library of diversely substituted α-acyl aminocarboxamides performing Ugi multicomponent reaction (U-4CR) out of four starting materials in a one-pot reaction.[26] In order to identify cellular targets, we synthesized biotin-linked versions of the most potent anti-HSF1 compounds and performed mass spectrometry-based affinity capture experiments.

Results and Discussion

Compound Synthesis

As can be seen in the Figure 1, currently reported HSF1 inhibitors of natural origin consist of a highly reactive Michael system which belongs to the so called pan-assay interference compounds (PAINS).[27-28] Those compounds are prone to react covalently with proteins. However, covalent binding to a certain target in cancer therapy might be eligible. E.g. the kinase inhibitors afatinib[29] and ibrutinib[30] were recently launched to the market. Thus, HSF1 inhibitors containing an α,β-unsaturated carbonyl moiety might be good starting point. Furthermore, studying the chemical scaffold of aforementioned HSF1-related compounds **1**–**9**[21-25] it becomes apparent that these substances possess a certain degree of bulkiness due to aromatic and saturated rings and diverse residual groups. Hence, we used the Ugi four-component reaction (U-4CR)[31] to establish a diversely substituted library. Beside 2,5-diketopiperazines,[32] this reaction gives easy access to broad range of α-acyl aminocarboxamides (**10** or **11**) in a single-step conversion using an aldehyde (**12**), and amine (**13**), an isocyanide (**14**) and a carboxylic acid (**15** or **16**) as reaction participants (Scheme 1).[31] Beside some polar functional groups being crucial for a balanced lipophilicity, various aliphatic substituted reactants were chosen for U-4CR to be able to increase the stereoscopic specificity and therefore the associated selectivity.[33] For that purpose, starting materials with aromatic moieties (phenyl, benzyl), aliphatic residues (methyl, propyl, butyl, pentyl, hexyl) and polar functional groups (furyl, morpholinyl, hydroxyl ether, methyl ether) were applied for the synthesis approach (Table 1).

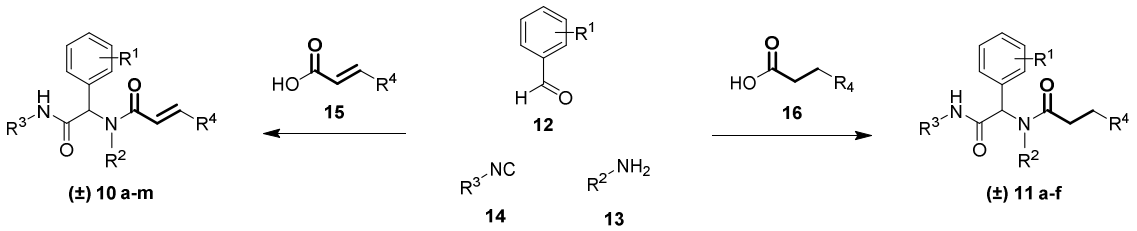

Scheme 1: The U-4CR gives access to a great variability of α-acyl aminocarboxamides (**10** or **11**) with and without an α,β-unsaturated carbonyl moiety (shown in bold, respectively) in only one synthesis step.
Reagents and conditions: **12** (1.0 equiv), **13** (1.0 equiv), **14** (1.2-1.3 equiv), **15** or **16** (1.0-1.3 equiv), abs. CH_3OH, r.t., 2 h-15 d, 36-81%.

At first the corresponding aldehydes (**12**) and amines (**13**) were pre-condensated in absolute CH_3OH. The concentrations of **12** and **13** ranged between 0.4 M and 1.2 M as it was reported that U-4CR ensure more effectiveness if the reactants are available in high concentration.[26] Corresponding isocyanides (**14**) and carboxylic acids (**15** or **16**) were added subsequently in a slight excess of 1.0 to 1.3 equiv and reacted to the α-acylaminocarboxamides **10a-m** and **11a-g** at r.t (Table 1). Some products (e.g. **10a**, **10b**, **10c**, **10e**, **11b**, **11c**) precipitated after short reaction time and were isolated by filtration and recrystallization in good yields. The products **11a** and **11d-g** were purified by means of medium pressure liquid chromatography (MPLC) and were obtained in moderate yields.

After preliminary evaluation of the inhibitory effect of these compounds (data not shown), the two most potent compounds **10b** and **10j** were structurally modified to analyse the effect of the bromo-substituent R^1 at the phenyl residue on the one hand and the effect of the highly reactive enone function on the other hand (Scheme 1). **10l** and **10m** are the bromoless analogues of **10b** and **10j**, respectively, and were synthesized by using the benzaldehyde instead of 2-bromo-benzaldehyde. Compounds **11a** and **11b** are analogous to **10l** and **10m** and were obtained by

means of hydrocinnamic acid and 3-(2,4-dichlorophenyl)propionic acid instead of the corresponding unsaturated derivatives, respectively (Table 1).

Table 1: Synthesised series of α-acyl aminocarboxamides with (**10a-m**) and without (**11a-g**) α,β-unsaturated carbonyl moiety**.**

product	R^1	R^2	R^3	R^4	[%]
(±) **10a**	2-Br	Me	Bn	Ph	77
(±) **10b**	2-Br	*c*-Propyl	Bn	Ph	57
(±) **10c**	2-Br	Bn	Bn	Ph	75
(±) **10d**	2-Br	4-MeO-Bn	Bn	4-MeO-Ph	60
(±) **10e**	2-Br	*n*-Propyl	*c*-Hexyl	4-MeO-Ph	72
(±) **10f**	2-Br	Furan-2-yl-methyl	*c*-Hexyl	Me	81
(±) **10g**	2-Br	3,4-$(MeO)_2$-phenethyl	*n*-Pentyl	H	61
(±) **10h**	2-Br	2-Cl-Bn	*t*-Butyl	Me	69
(±) **10i**	2-Br	2-(2-Hydroxyethoxy)ethyl	*t*-Butyl	H	41
(±) **10j**	2-Br	Bn	2-Morpholinoethyl	2,4-$(Cl)_2$-Ph	36
(±) **10k**	2-Br	*n*-Propyl	2-Morpholinoethyl	Ph	37
(±) **10l**	H	*c*-Propyl	Bn	Ph	73
(±) **10m**	H	Bn	2-Morpholinoethyl	2,4-$(Cl)_2$-Ph	53
(±) **11a**	2-Br	*c*-Propyl	Bn	Ph	60
(±) **11b**	2-Br	Bn	2-Morpholinoethyl	2,4-$(Cl)_2$-Ph	62
(±) **11c**	4-Br	*c*-Propyl	Bn	Ph	66
(±) **11d**	4-OH	*c*-Propyl	Bn	Ph	80
(±) **11e**	4-(2-Bromoethoxy)	*c*-Propyl	Bn	Ph	67
(±) **11f**	4-Br	*c*-Propyl	Bn	4-Hydroxyphenyl	77
(±) **11g**	4-(2-Bromoethoxy)	*c*-Propyl	Bn	4-Hydroxyphenyl	73

For the identification of cellular drug targets by means of affinity capture experiments, three different biotin-labelled compounds (**20**, **22**, **24**) were prepared (Scheme 2 and 3). First of all, 4-(2-bromoethoxy)benzaldehyde (**17**) was prepared according to Jiang

and colleagues.[34] Condensation of **17**, *c*-propylamine, benzyl isocyanide and 3-(4-hydroxyphenyl)propionic acid gave **11g**, which was reacted with 2,2´-(ethylenedioxy)bis(ethylamine) and basic K_2CO_3 to give **21**. Subsequently, **21** was biotinylated to achieve **22** which was purified by means of reversed phase MPLC. The synthesis of compound **20** is analogous.

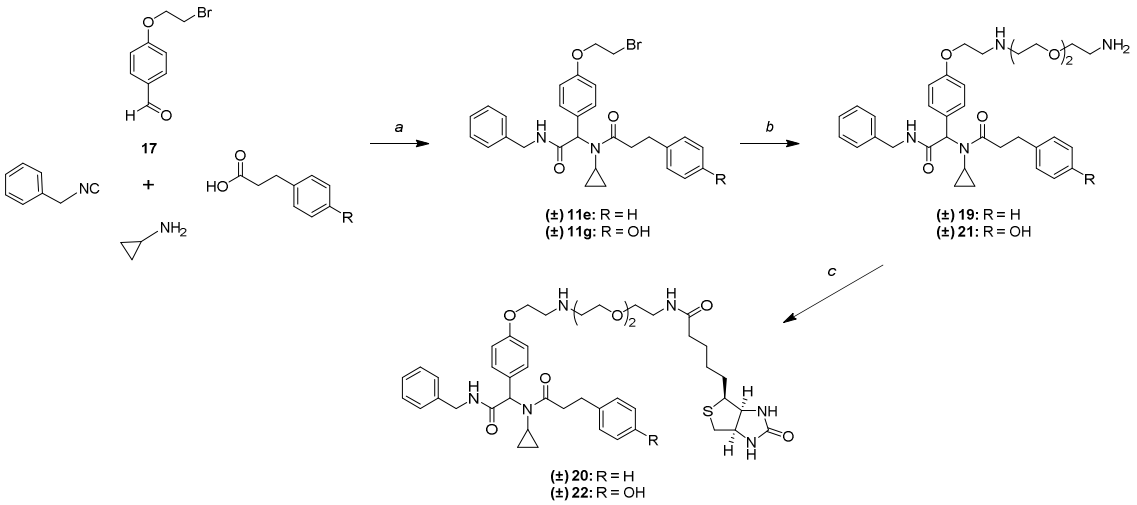

Scheme 2: Synthesis route to the biotinylated compounds **20** and **22** which were used for the affinity capture experiment
Reagents and conditions: a) abs. CH_3OH, r.t., 16 h; *b)* 2,2´-(ethylenedioxy)bis(ethylamine), K_2CO_3, abs. CH_3CN, 80 °C; 3-6 h; *c)* NHS-Biotin, DIPEA, abs. DMF, r.t., 16-24 h.

The synthesis of biotin-labelled compound **24** started off by substitution of **11f** (Scheme 3) with 1,4-dibromobutane in presence of K_2CO_3. The obtained compound **18** was converted with 2,2´-(ethylenedioxy)bis(ethylamine) including K_2CO_3 and biotinylated by means of *N*,*N*-Diisopropylehtylamine and NHS-Biotin in absolute DMF. Purification by reversed phase MPLC gave compound **24**.

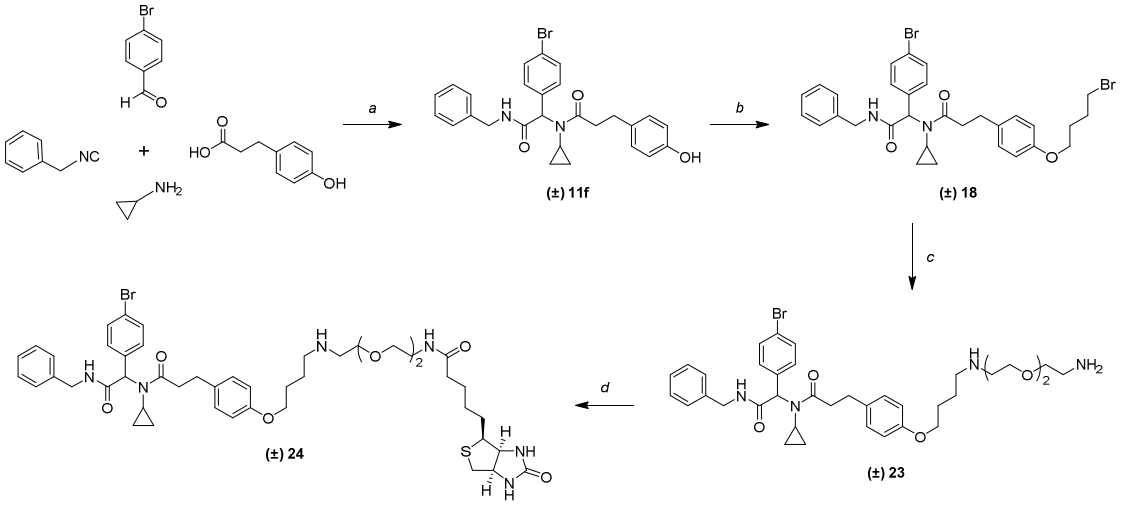

Scheme 3: Synthetic route of the biotinylated compound **24** for the affinity capture experiment.
Reagents and conditions: *a)* abs. CH_3OH, r.t.; *b)* 1,4-dibromobutane, K_2CO_3, abs. CH_3CN, 100 °C, 3 h; *c)* 2,2´-(ethylenedioxy)bis(ethylamine), K_2CO_3, abs. CH_3CN, 100 °C, 4 h; *d)* NHS-Biotin, DIPEA, abs. DMF, r.t., 22 h.

Structure-HSF1-dependent HSR activity relationship analysis

The isolated α-acyl aminocarboxamide products were tested in a recently established biological HSR model assay for their ability to inhibit the HSF1-mediated upregulation of the heat shock proteins HSP72 and HSP27 upon cellular stress.[16] In brief, INA-6 MM cells were pre-treated with the compounds **10a-m, 11a-g** and **18-24** (used concentrations: **23** 12.5 μM, **19** 25 μM, and all others 50 μM), respectively, prior to incubation with the pharmacological HSP90 inhibitor and HSR inducer NVP-AUY922 (**25**),[35] harvested and analysed for HSP72, HSP27, HSF1 or phospho-HSF1 expression by Western blot (Figure 2). Of note, this cellular assay requires that a tested compound can pass the cell membrane**.** For detection of HSP72 protein, the main HSR readout marker, two complementary assays were employed using the same protein lysate: Western blot analysis as a semi-quantitative method (Figure 2), and ELISA for quantitative analysis of the HSP72 protein expression (Figure 3). In addition, HSP72 mRNA level were determined for selected active or inactive

compounds to investigate whether HSP72 induction is mediated by HSF1-mediated transcription (Figure 4).

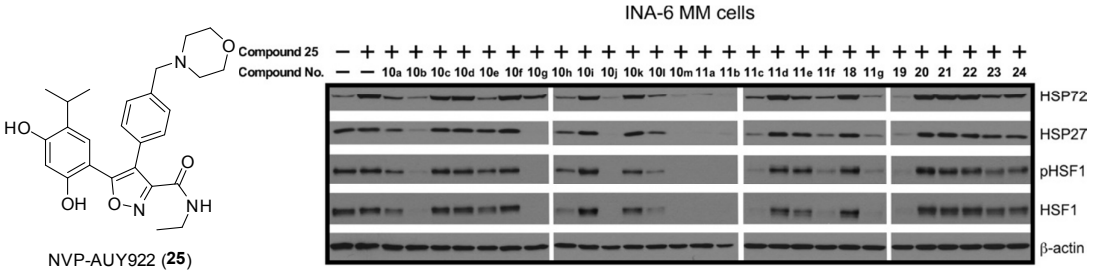

Figure 2: Western blot analyses of HSF1 expression or HSF1 phosphorylation at the Serine residue 326, or of HSF1-dependent induction of the heat shock proteins HSP72 or HSP27. INA-6 MM cells were incubated with the compounds **10a**-**m**, **11a-g** or **18-24** for 4 hours, and concomitantly treated with the compound **25** (to induce HSF1 activity by inhibition of HSP90) for additional 4 h. INA-6 cells treated only with DMSO or with the compound **25** served as negative or positive controls, respectively. Staining of β-actin served as a control for equal loading.

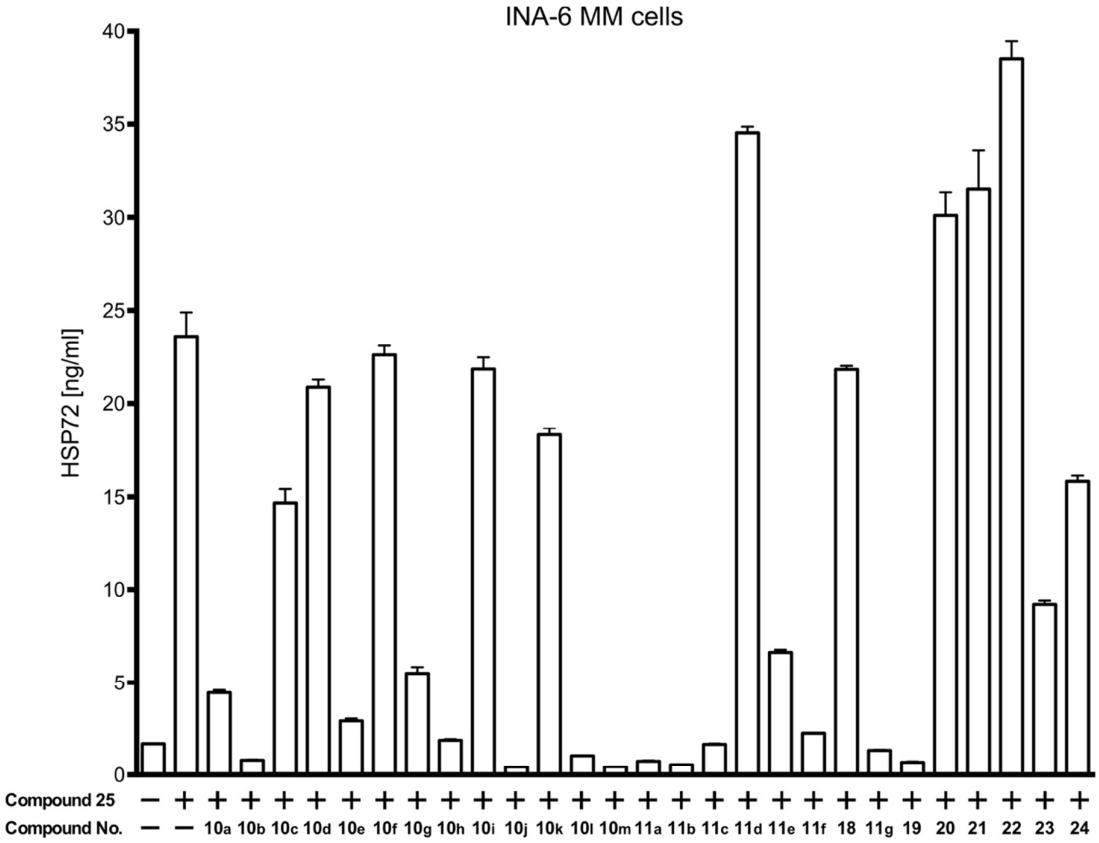

Figure 3: Quantitative analysis of HSP90 inhibition-induced, HSF1-dependent HSP72 expression using an ELISA assay. INA-6 cells were incubated with the compounds **10a-m, 11a-g** or **18-24** for 4 h, followed by HSF1 stimulation through co-treatment with the HSP90 inhibitor compound **25** for additional 4 h. INA6 cells treated

with DMSO or with compound **25** alone served as negative or positive controls, respectively.

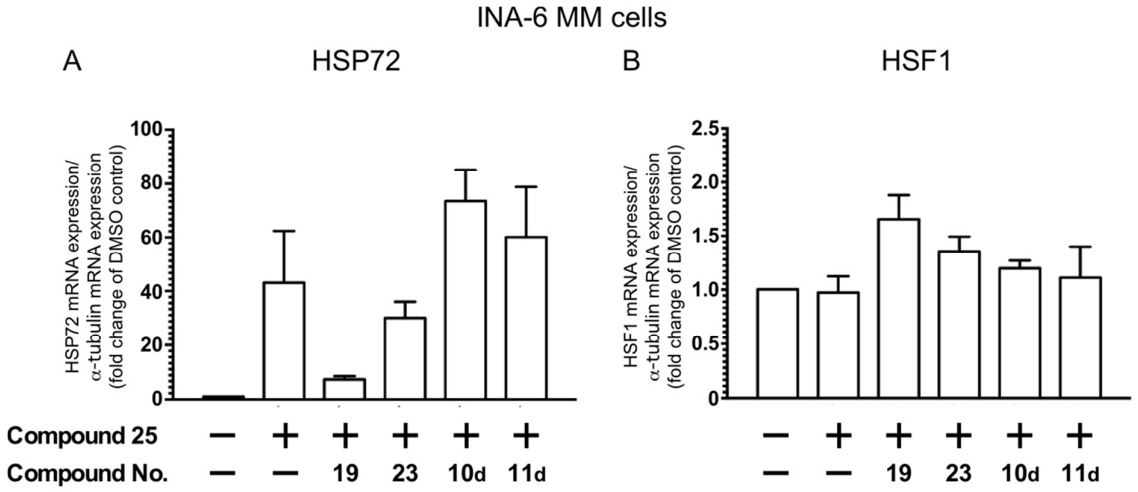

Figure 4: Transcriptional changes in the expression of HSP72 and HSF1. INA-6 cells were treated with the compounds **19** (25 µM), **23** (12.5 µM), **10d** (50 µM) and **11d** (50 µM) for 4 h and were co-treated with 10 nM of **25** for an additional 4 h. Afterwards, total RNA was isolated and gene expression of HSP27, HSP72 and HSF1 was measured by real-time PCR. Data are normalized against α-tubulin. Shown are means and standard deviations of three independent experiments.

With regard to the initially synthesized Michael-acceptor compounds **10a**–**m** the induction of HSP72 or HSP27 expression by **25** was completely abrogated by **10b**, **10j** and **10m** and strongly suppressed by **10a**, **10e**, **10g**, **10h** and **10l,** whereas **10c**, **10d**, **10f, 10i** and **10k** had only moderate or no effect. Perfectly in line with the HSP72 Western blot results, the findings from the ELISAs illustrate that pre-treatment with compounds **10c**, **10d**, **10f**, **10i** and **10k** show no or only minor effects on the amount on induced HSP72. In contrast, treatment with the α-acyl aminocarboxamides **10a**, **10b**, **10e**, **10g**, **10h**, **10j, 10l** and **10m** significantly prevented induction of HSP72 or HSP27. The strongest inhibitory effect was observed for compounds **10b**, **10j, 10l** and **10m** which show a HSP72 or HSP27 level comparable to unstressed cells indicating a sufficient suppression of HSF1 function. As **10l** and **10m** are the bromoless derivatives of **10b** and **10j**, respectively, the bromo-substituent R^1 in the ortho position is not crucial for the inhibitory activity. However, among the compounds **10a**-**m** the potency to inhibit the HSF1-dependent

HSP72/HSP27-upregulation was unaffected by their respective structural alteration, and thus no obvious structure-HSF1 activity relationship could be derived.

For the investigation of the effect of the Michael system the compounds **10b** and **10j** were compared to the saturated analogues **11a** and **11b**. Western blot and ELISA analysis show similar induction of HSP72 expression so that the effect of the α,β-unsaturated carbonyl moiety and the related covalent binding to the target are unlikely. The compounds **11c** and **11d** differ in the para substituent R^1 with **11d** carrying an OH group. ELISA analysis show strong induction effect of **11c** but no effect for **11d,** indicating that a hydrogen bond donor at this molecule residue is not crucial for the inhibitory effect. Concurrently, a hydrogen bond acceptor with a short linker at R^1 is tolerable as the compound **11e** shows moderate activity. At the residue R^4 compound **11f** carries an additional hydrogen bond donor in comparison to **11c**. Both compounds show the same activity pointing to the unimportance of the phenolic OH group. However, replacement of the OH substituent with a bromobutoxy group at R^4 reduced the inhibitory effect. Of note the compound **11g** consisting of the bromoethoxy group in the position R^1 (cf. **11e**) and the phenolic OH group in the position R^4 (cf. **11f**) belongs to the most active substances of the library.

The biotinylated compounds **20**, **22** and **24** and their intermediates **19**, **21** and **23** were tested for the ability to inhibit the HSF1-mediated upregulation of HSP72 or HSP27, as well. Because the substances **19-24** are quite large molecules with molecular weight up to 940 g/mol and many hydrophilic residues, we supposed that their membrane permeability to the cell cytosol might be hindered. With the exception of substance **19,** this hypothesis was confirmed by Western blots as well as by ELISA analyses.

In order to analyze potential mechanisms underlying the suppression of HSP72 and HSP27, we additionally determined HSF1 and phospho-HSF1 protein expression by

Western blot, and HSF1 mRNA level by RT-PCR. Western blot analyses revealed downregulation of both HSF1 and phospho-HSF1 protein level only upon treatment with the anti-HSR-active compounds (Figure 2), whereas HSF1 mRNA, as detected by RT-PCR, remained unaffected for all compounds tested (Figure 4). This result suggests that impairment of HSF1 protein stabilization or HSF1 mRNA translation rather than inhibition of HSF1 transcription or HSF1 protein activation are potential mechanisms underlying the observed anti-HSR effects of the active compounds. Our finding is in a good accordance with a previous report showing downregulation of HSF1 after PI3 kinase inhibition.[13]

Drug Target Identification

In order to identify cellular drug targets of compounds that efficiently inhibit HSF1-dependent heat shock response, the biotin-labelled compounds **20**, **22** and **24** (Scheme 2 and 3) were applied for affinity capture experiments using streptavidin magnetic beads in combination with quantitative mass spectrometry. To distinguish between specific and unspecific binders, empty streptavidin beads were used as a control. Compound-loaded beads and control beads were incubated with INA-6 cell lysate under the same conditions. After washing, proteins were eluted, digested with trypsin and analysed by nanoLC-MS/MS. Protein intensity ratios between inhibitor and control samples were calculated for all identified proteins by label-free quantification (Figure 5).

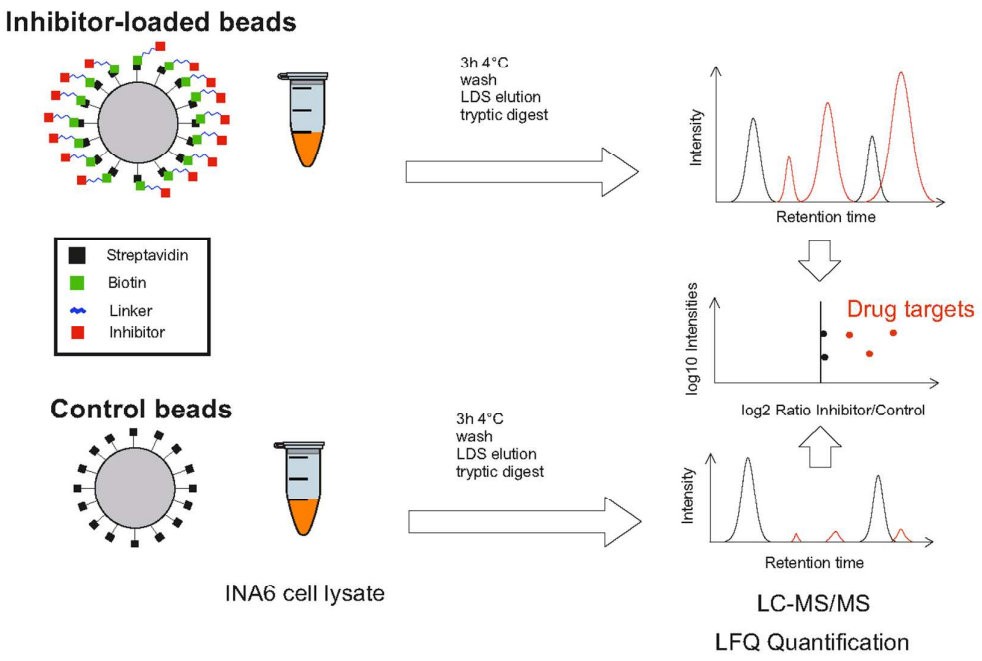

Figure 5: Workflow of the affinity capture experiment. Biotinylated inhibitor was loaded on streptavidin beads; empty beads were used as control. Both beads were incubated with INA-6 cell lysate for 3 h at 4 °C, washed, and captured proteins were eluted with LDS sample buffer. Proteins were digested with trypsin and analyzed by nanoLC-MS/MS. Label-free quantification (LFQ) of both samples was performed for all identified proteins.

The result of the analysis of five biological replicates for compound **22** is shown in Figure 6A. All quantified proteins are listed in Supplemental Table S1. In summary, we identified 68 proteins that are significantly enriched with inhibitor-loaded beads over the control. The enriched proteins are a mixture of direct drug targets and protein-protein interaction partners thereof, and it is not possible from the present data to distinguish between those. A number of protein complexes are specifically enriched with the compound **22**: the MICOS complex, which regulates mitochondria morphology and protein transport,[36] four subunits of the SMN complex, which has an essential role in the assembly of the splicesosomal small nuclear ribonucleoproteins (snRNPs),[37] and six subunits of the CCR4-NOT complex, which is among other things involved in the DNA damage response.[38] In addition, we identified a number of

peroxisomal proteins; proteins associated with apoptosis, such as MAP3K5, MAP3K6, PDCD6 and PEF1, five subunits of phosphatase 6, an enzyme involved in mitosis and cell cycle progression.[39] Interestingly, we identified four members of the phosphatidylinositol 3-kinase-related kinases (PIKK), namely DNA-PK (PRKDC), ATM and ATR which are involved in the DNA damage response (DDR) and interact with each other,[40] and mTOR which regulates cell growth by modulating many processes including protein synthesis, ribosome biogenesis and autophagy.[41-42] Beside its role in the DDR, DNA-PK interacts with HSF1[43] and it was shown that the DNA-PK is important for the HSF1-mediated upregulation of HSP72 during the heat shock response (HSR).[44]

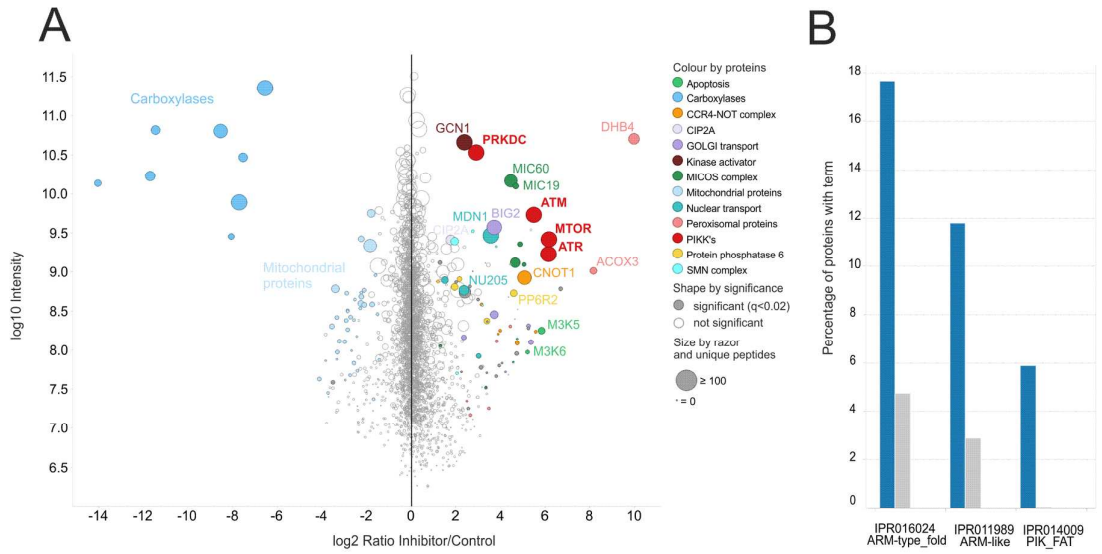

Figure 6: A) Identification of potential drug targets from affinity capture experiments with **22** and INA-6 cell lysate. Proteins significantly enriched (Benjamini-Hochberg adjusted limma p-value < 0.02) over control are represented by closed circles. Protein ratios and intensities are median values from five biological replicates (n replicates > 1). The size of the circles correlates with the number of identified razor and unique peptides. Proteins from the same complex, the same protein family or with a similar function are marked in the same color. Carboxylases were enriched specifically with the streptavidin control beads as they have Biotin as prosthetic group. **B)** Significantly enriched, non-redundant InterPro domains (Benjamini-Hochberg adjusted Fisher´s exact test p-value < 0.01). Blue bars show fraction of terms present in significantly enriched proteins (Benjamini-Hochberg adjusted limma

p-value < 0.02, n replicates > 1 and log2 ratio > 0) (drug targets) or in not significantly enriched proteins (grey bars, unspecific proteins).

In order to find a common theme among these various proteins with diverse biological functions, we performed an enrichment analysis for protein domains (Figure 6B). The most common protein domain, found in more than 17% of the potential drug targets, is the armadillo domain (ARM). Within the 68 potential drug targets we identified 13 proteins (PRKDC, ATM, ATR, MTOR, XPOT, PP6R1, PP6R2, MON2, CIP2A, CNOT1, RCD1, GCN1, BIG2) containing the armadillo domain which is composed of several variable helical repeats forming a superhelix that is important for protein-protein interaction.[45]

These 13 armadillo domain-containing proteins - together with their high confident interaction partners listed in the HitPredict database[46] - cover most of the 68 potential drug targets identified by our affinity capture approach (Supplemental Table S1). Thus, it is tempting to speculate that the armadillo domain is the primary target of the investigated α-acyl aminocarboxamides. Although this domain differs from protein to protein in repeat-length, it was shown by Dahlstrom and coworkers that the peptide binding site contains binding pockets with highly conserved residues.[47]

In addition to affinity capture experiments with compound **22,** we analyzed the compound with a different linker position **24** (Scheme 2 and 3) with the same strategy. The potential cellular targets identified from these two compounds largely overlap (Supplemental Figure S6). Especially, the PIKKs are identified in both experiments as drug targets indicating that neither the linker position of compound **22** nor the linker position of compound **24** is essential for binding to PIKKs. However, for a few protein complexes the linker position seems to interfere with protein binding. E.g. the linker position of **24** seems to interfere with binding of CCR4-NOT complex, and the linker position of **22** seems to interfere with binding of the COG complex

(Supplemental Figure S6). Consistently, affinity capture experiments with compound **20** indicated that the absence of the phenolic hydroxyl moiety of **22** does not significantly influence drug target binding (data not shown).

In order to validate some of the MS data, we performed Western blot analyses of the INA-6 MM cell eluates using specific antibodies against the PIKKs DNA-PK, ATM, ATR or mTOR. As compared to the control approach, all PIKKs were significantly higher detectable in the cell eluate that had been incubated with the beads-labelled compound **22** (Figure 7).

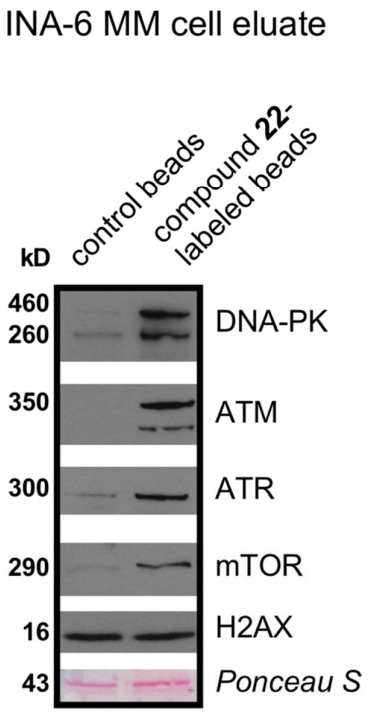

Figure 7: Shown are Western blot analyses of the PI3 kinase-related kinases (PIKKs) DNA-PK ATM, ATR and mTOR upon incubation of INA-6 cell lysates either with compound **22**-coupled beads or with beads only as a control. Staining against H2AX or Ponceau S served as loading controls.

Anti-tumor activity

Next, we aimed to evaluate potential anti-tumor effects of the anti-HSF1-suppressive compounds, and analyzed tumor cell survival in the MM cell line model INA-6. Cells

were treated either with DMSO as a solvent control or with increasing concentrations of the compounds **19**, **23** or **10d**, respectively, for three days prior to viability assessment by annexin V-FITC/propidium iodide staining and measurement by flow cytometry. Based on the detected viable cell fractions, which are negative for both annexin V and propidium iodide, dose-response curves of three independent experiments were calculated using GraphPad Prism software. As shown in Figure 8, treatment with the both anti-HSR-active compounds **19** and **23** strongly reduced INA-6 cell viability by induction of apoptotic cell death within a low micromolar concentration range (8.6 µM and 6.3 µM, respectively) (Figure 8A and B), whereas the anti-HSR-inactive compound **10d** had no effect on cellular viability (Figure 8C).

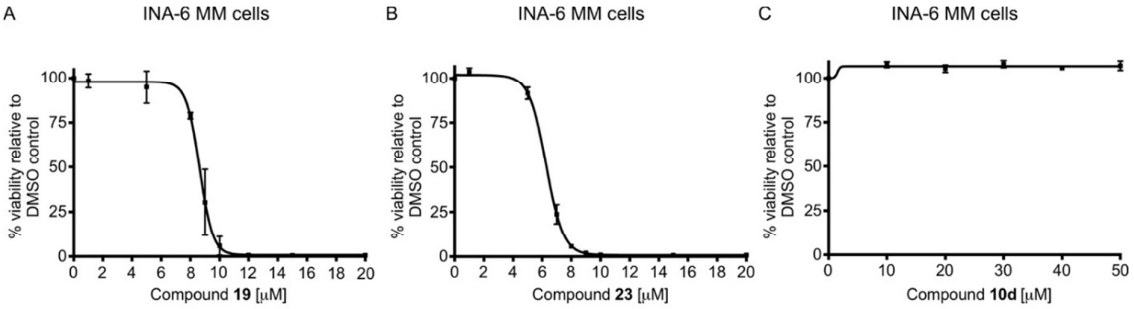

Figure 8: Viability analysis of INA-6 MM cells upon treatment with the compounds **19** (A), **23** (B) or **10d** (C). INA-6 cells were incubated either with DMSO as a solvent control or with increasing concentrations of the compounds **19**, **23** or **10d** for three days prior to viability assessment by annexin V-FITC/ propidium iodide staining and measurement by flow cytometry. Shown are mean values and standard deviations of three independent experiments.

In addition, we aimed to evaluate potential synergistic effects of an anti-HSR-active compound and the HSP90 inhibitor **25**, and performed a combination experiment. INA-6 cells were incubated with sub-maximally effective concentrations either of the compound **19** (for 72 h), the HSP90 inhibitor **25** (for 68 h), or a combination of both compounds prior to viability analysis. As shown in Figure 9, we observed a strong synergistic apoptotic effect of the combination approach, which strengthens our

hypothesis that concomitant inhibition of the HSR might trigger apoptotic effects HSP90 inhibitors.

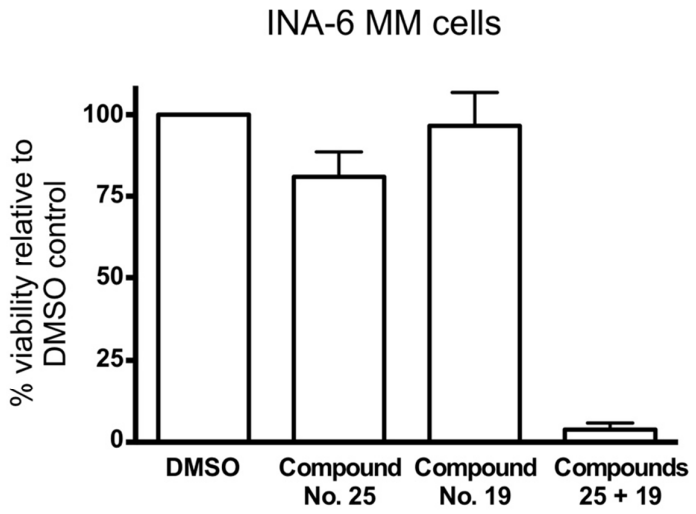

Figure 9: Combined inhibition of HSP90 and HSF1-dependent heat shock response (HSR). INA-6 cells were incubated with sub-maximally effective concentrations either of the compound **19** (for 72 h), the HSP90 inhibitor **25** (for 68 h), or a combination of both compounds. 4 h after the treatment start with either with DMSO as a solvent control or compound **19**, either DMSO or 10 nM of **25** were added for an additional 68 h followed by flow cytometry-based viability analysis (annexin V-FITC/ propidium iodide staining). Data show the means and the standard deviations of the viable cell fractions based on three independent experiments. Percentages were calculated relative to the respective DMSO-treated controls.

Since MS-based target search revealed several PIKKs as potential targets of our active compounds, we finally wanted to evaluate the role of DNA-PK and mTOR, two PIKK family members, for HSF1-mediated HSR using the dual DNA-PK/mTOR inhibitor NU7441 (**26**).[48] INA-6 cells were treated with the dual DNA-PK/mTOR inhibitor **26** (10 µM) for 4 h and were co-treated with 10 nM of **25** for an additional 4 h prior to analyses of HSF1, phospho-HSF1, HSP72 or HSP27 proteins by Western blot (Figure 10A), or the mRNA expression level of HSF1 or HSP72 by RT-PCR (Figure 10B). Both analyses show similar results regarding the HSF1-dependent HSR suppression as compared to our anti-HSR active compounds underscoring their

proposed mode of action, namely blockage of HSP90 inhibitor-dependent HSP72 induction on mRNA and protein level as well as HSF1 and phospho-HSF1 downregulation. The similar observation of HSF1 downregulation upon both treatment approaches, either with the dual DNA-PK/mTOR inhibitor or with our active compounds, indicates involvement of common mechanisms affecting translation of mRNA into protein or protein stability but not transcriptional or phosphorylation-mediated activation of HSF1.

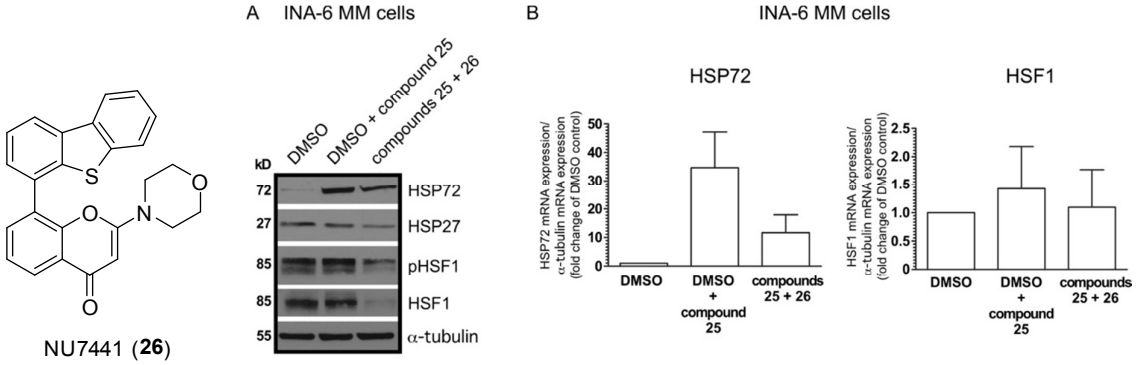

Figure 10: Dual DNA-PK/mTOR inhibition blocks HSF1-dependent HSR upon HSP90 inhibition. INA-6 cells were treated with the dual DNA-PK/mTOR inhibitor **26** (10 µM) for 4 h and were co-treated with 10 nM of **25** for an additional 4 h. Afterwards, protein as well as total mRNA were isolated. Expression level of HSF1, phospho-HSF1, HSP72 or HSP27 were analyzed by Western blot. Staining of a-tubulin served as a loading control (A). The mRNA expression level of HSF1 or HSP72 were determined by RT-PCR. Data were normalized against α-tubulin. Results are means and standard deviations of three independent experiments (B).

Conclusion

Experimental data suggests that HSF1 is critically involved in pathological processes, e.g. of neurodegenerative diseases or cancer.[3-4,49] We have recently established the critical role of HSF1 for the protective up-regulation of HSP72 expression in MM, in particular upon exposure to therapeutic agents that increase proteotoxic stress, like the HSP90 inhibitor **25** or the proteasome inhibitor bortezomib. As this mechanism distinctly contributes to the survival of MM cells, it is regarded to play an essential role in the observed drug-resistance in the treatment of Multiple Myeloma.[16] However, from a clinical perspective, the translation of direct therapeutic targeting of HSF1 as a therapeutic principle into clinical trials is currently hampered, mainly due to the shortage of clinically suitable pharmacological inhibitors. Therefore, the aim of this study was the development of potent and selective inhibitors of the HSF1-dependent HSR (for combined approaches with stress-inducing agents).

Utilizing the well-known Ugi multicomponent reaction a smart library of structurally diverse compounds was synthesized and their potential to inhibit the HSF1 activity was tested. Monitoring the HSF1-dependent induction of HSP72 and HSP27 expression using the HSP90 inhibitor **25** revealed two very potent inhibitors bearing a highly reactive Michael system and a bromophenyl ring. Omission of both moieties resulted in equally potent HSF-1 inhibitors indicating that both groups are not necessary for inhibitory activity. Thus, the compounds **11a** and **11b** as well as **19** can be regarded as excellent lead structures for further optimization.

Additional functional analyses revealed that the observed anti-HSR effect of these active compounds is neither the result of a functional inactivation by inhibition of HSF1 phosphorylation, nor caused by transcriptional downregulation. In fact, treatment with the active compounds resulted in a loss of total HSF1 protein

expression indicating destabilization of HSF1 protein or impaired translation of HSF1 mRNA into HSF1 protein as potential underlying mechanisms.

We identified members of the PIKK family, namely DNA-PK, ATM, ATR and mTOR as strong candidates for primary and therapeutically relevant targets. Beside their role in the DNA damage response,[40] it has been reported that DNA-PK is involved in the HSF1-mediated upregulation of HSP72[44] and might therefore represent a significant therapeutic point of attack. In line with this assumption, we here could mimic the anti-HSR effects of our active compounds using a dual DNA-PK/mTOR inhibitor.

Yet, HSF1 remains an important therapeutic target for drug development as recent HSF1 phenotypic screens by the Workman group led to potent novel inhibitors additionally targeting CDK9 and Pirin.[19-20]

Experimental

Chemistry: *General Methods for Synthesis:*

Melting points were determined on a Stuart melting point apparatus SMP11 (Bibby Scientific, UK) and Melting point meter MPM-H2 (Schorpp Geraetetechnik, Ueberlingen, Germany) and were not corrected. IR spectra were obtained using a JASCO FT/IR-6100 spectrometer (JASCO, Gross-Umstadt, Germany). TLC was performed on pre-coated aluminium sheets with silica gel 60 F_{254} and pre-coated aluminium sheets with silica gel C_{18} F_{254} (Macherey-Nagel, Dueren, Germany). ^{1}H (400 MHz) and ^{13}C (100 MHz) NMR spectra were recorded on a Bruker AV 400 instrument (Bruker Biospin, Ettlingen, Germany). Chemical shifts are given in ppm and were calibrated on residual solvent peaks as internal standard (C_6D_6: ^{1}H 7.15 ppm, ^{13}C 128.0 ppm; $CDCl_3$: ^{1}H 7.26 ppm, ^{13}C 77.1 ppm, CD_3CN: ^{1}H 1.94 ppm, ^{13}C 1.24 ppm[50]). NMR signals were specified as s (singlet), d (doublet), t (triplet), m (multiplet), bs (broad singlet), dd (doublet of doublets), dt (doublet of triplets). Coupling constants *J* are given in Hz. Medium pressure liquid chromatography (MPLC) was performed on puriFlash®430 system (Interchim, Montluçon, France) using pre-packed silica gel 50µ columns from Interchim (Montluçon, France). Reversed phase MPLC was performed using pre-packed C18-HQ silica gel 15µ columns from Interchim (Montluçon, France) and HPLC grade solvents from Sigma-Aldrich Chemie GmbH (Munich, Germany). MS data were obtained using an Agilent 1100 Series LC/MSD Trap (Agilent Technologies, Boeblingen, Germany). Purity of substances **10a-m**, **11a-g**, **18**, **19** and **21-23** was determined by a chromatographic method (HPLC) and found to be > 95%. The purity of substances **20** and **24** was determined by absolute qNMR according to ACS instruction to purity determination

and found to be > 91% and >88%, respectively. Commercial available chemicals were used without further purification.

*General procedure for the synthesis of the α-acyl aminocarboxamides **10a-m, 11a-g**.*

To a solution of the respective benzaldehyde (1.0 equiv) in absolute CH_3OH the corresponding amine (1.0 equiv) was added under Argon atmosphere and stirred for 20 min at r.t. Then the isocyanide compound (1.2-1.3 equiv) and the corresponding acid derivative (1.0-1.3 equiv) were added. The solution stirred until the reaction, controlled by means of TLC, was finished. The particular compounds were purified either by filtration and crystallization or by means of chromatographic purification methods. Detailed synthesis procedures and structure characterization data of **10a-m** and **11a-g** are described in the Supplemental Information.

4-(2-bromoethoxy)benzaldehyde (**17**) was prepared according to Jiang and colleagues[34]: 4-hydroxybenzaldehyde (1.99 g, 16.2 mmol) was dissolved in absolute CH_3CN (50 mL). K_2CO_3 (4.50 g, 32.5 mmol) and 1,2-dibromoethane (14.1 mL, 164 mmol) were added and the reaction mixture refluxed 24 h at 90 °C. The reaction mixture was filtered and the filtrate was concentrated *in vacuo*. After the purification by MPLC (petroleum ether/EtOAc 4/1 to 1/1) **17** was obtained as colourless solid (3.26 g, 87%). ^{1}H NMR ($CDCl_3$, 400 MHz): δ 9.90 (s, 1H), 7.85 (d, *J*=8.8 Hz, 2H), 7.02 (d, *J*=8.7 Hz, 2H), 4.38 (t, *J*= 6.2 Hz, 2H), 3.67 (t, *J*=6.2 Hz, 2H); ^{13}C NMR ($CDCl_3$, 100 MHz): δ 190.7, 163.0, 132.1, 130.5, 114.9, 68.0, 28.5; mp 52-53 °C.

N-(2-(benzylamino)-1-(4-bromophenyl)-2-oxoethyl)-3-(4-(4-bromobutoxy)phenyl)-N-cyclopropylpropanamide (**18**): **11f** (300 mg, 0.59 mmol) was dissolved in absolute CH_3CN (6.0 mL) under Argon atmosphere. K_2CO_3 (166 mg, 1.20 mmol) and 1,4-dibromobutane (700 µL, 5.83 mmol) were added and the reaction mixture refluxed 3 h at 100 °C. Afterwards the suspension was filtered, the filtrate

concentrated *in vacuo* and purified by MPLC (petroleum ether/EtOAc 4/1 to 1/4) to obtain **18** as colourless solid (261 mg, 70%). ^{1}H NMR ($CDCl_3$, 400 MHz): δ 7.43 (m, 2H), 7.35-7.25 (m, 5H), 7.16-7.12 (m, 4H), 6.81 (m, 2H), 6.51 (t, *J*=5.6 Hz, 1H, NH), 5.59 (s, 1H), 4.46 (m, 2H), 3.99 (t, *J*=6.0 Hz, 2H), 3.51 (t, *J*=6.6 Hz, 2H), 2.97-2.84 (m, 4H), 2.51-2.46 (m, 1H), 2.13-2.06 (m, 2H), 1.99-1.92 (m, 2H), 0.95-0.90 (m, 1H), 0.86-0.80 (m, 1H), 0.71-0.60 (m, 2H); ^{13}C NMR ($CDCl_3$, 100 MHz): δ 176.3, 169.7, 157.4, 138.1, 134.8, 133.3, 131.6 (2C), 130.8 (2C), 129.5 (2C), 128.7, 127.6, 127.4, 122.1, 114.5 (2C), 66.9, 65.8, 43.7, 36.5, 33.5, 31.2, 30.4, 29.5, 28.0, 10.6, 9.3; IR $\tilde{\nu}$ 3252, 3065, 2925, 1642, 1512, 1397, 1246, 1071, 1011, 822, 700 cm^{-1}; ESI-MS: *m/z* 642.9 [M+H^{+}]; mp. 112-113 °C.

N-(1-(4-(2-((2-(2-(2-aminoethoxy)ethoxy)ethyl)amino)ethoxy)phenyl)-2-(benzylamino)-2-oxoethyl)-N-cyclopropyl-3-(4-hydroxyphenyl)propanamide (**21**): **11g** (496 mg, 0.90 mmol), K_2CO_3 (149 mg, 1.08 mmol) and 2,2´-(ethylenedioxy)bis(ethylamine) (660 µL, 4.50 mmol) were suspended in absolute CH_3CN (4.5 mL) under Argon atmosphere. The reaction mixture refluxed 3 h at 80 °C. After the suspension was filtered, the filtrate was concentrated *in vacuo* and the crude product was purified by MPLC (EA/EtOH/NEt_3 1/1/0.1) to isolate **21** as yellowish oil (490 mg, 88%). ^{1}H NMR ($CDCl_3$, 400 MHz): δ 7.29-7.19 (m, 5H), 7.03-7.01 (m, 2H), 6.92-6.90 (m, 2H), 6.75-6.73 (m, 2H), 6.46-6.60 (m, 3H, NH), 5.43 (s, 1H), 4.48-4.36 (m, 2H), 4.10-4.01 (m, 2H), 3.63-3.58 (m, 6H), 3.53-3.51 (m, 2H), 3.00 (t, *J*= 5.13 Hz, 2H), 2.91-2.79 (m, 8H), 2.34-2.29 (m, 1H), 0.94-0.73 (m, 2H), 0.69-0.58 (m, 2H); ^{13}C NMR ($CDCl_3$, 100 MHz): δ 176.3, 170.5, 158.4, 155.7, 138.3, 131.5, 130.6, 129.6, 128.6, 127.9, 127.6, 127.3, 115.4, 114.4, 72.3, 70.4, 70.2, 70.1, 67.2, 66.3, 49.1, 48.5, 43.7, 41.2, 36.0, 31.3, 30.5, 10.3, 9.7; IR $\tilde{\nu}$ 3300, 2865, 1646, 1510, 1453, 1240, 1100, 1047, 828, 555 cm^{-1}; ESI-MS: *m/z* 619.2 [M+H^{+}].

N-(2-(2-(2-((2-(4-(2-(benzylamino)-1-(N-cyclopropyl-3-(4-hydroxyphenyl)propanamido)-2-oxoethyl)phenoxy)ethyl)amino)ethoxy)ethoxy)ethyl)-5-((3aS,4S,6aR)-2-oxohexahydro-1H-thieno[3,4-d]imidazol-4-yl)pentanamide (**22**): NHS-Biotin (40.0 mg, 0.12 mmol) was dissolved in absolute DMF (1.5 mL) under Argon atmosphere. Solution of **21** (87.0 mg, 0.14 mmol) and DIPEA (51.0 µL, 0.28 mmol) in absolute DMF (1.5 mL) was added dropwise and the reaction mixture stirred 24 h at r.t. After the solvent was removed *in vacuo* the crude product was directly purified by reversed phase MPLC (H_2O/ CH_3OH 8/2 to 1/9) to isolate **22** as a colourless solid (45.0 mg, 38%). ^{1}H NMR ($CDCl_3$, 400 MHz): δ 7.30-7.19 (m, 5H), 7.07-7.05 (m, 2H), 6.94-6.84 (m, 4H, 2 NH), 6.76-6.74 (m, 2H), 6.67-6.65 (m, 2H), 6.36 (d, *J*=5.1 Hz, 1H, NH), 5.55 (s, 1H, NH), 5.48 (d, *J*=3.0 Hz, 1H), 4.49-4.37 (m, 3H), 4.20-4.16 (m, 1H), 4.11-4.02 (m, 2H), 3.63-3.48 (m, 8H), 3.40-3.36 (m, 2H), 3.06-2.78 (m, 10H), 2.65-2.62 (m, 1H), 2.36-2.31 (m, 1H), 2.16 (t, *J*=7.4 Hz, 2H), 1.68-1.53 (m, 4H), 1.41-1.31 (m, 2H), 0.97-0.88 (m, 1H), 0.80-0.73 (m, 1H), 0.69-0.55 (m, 2H); ^{13}C NMR ($CDCl_3$, 100 MHz): δ 176.4, 173.8, 170.5, 164.0, 158.3, 155.4, 138.5, 131.8, 130.7, 129.6, 128.6, 128.1, 127.7, 127.3, 115.45, 114.4, 70.2 (2C), 70.1, 70.0, 67.2, 66.3, 61.9, 60.2, 55.6, 49.1, 48.6, 43.7, 40.5, 39.3, 36.1, 35.9, 31.2, 30.5, 28.3, 28.1, 25.6, 10.3, 9.8; IR $\tilde{\nu}$ 3288, 2924, 1686, 1644, 1511, 1453, 1238, 1100, 1029, 828, 576 cm^{-1}; ESI-MS: *m/z* 845.2 [M+H$^+$]; mp. 67-69 °C.

3-(4-(4-((2-(2-(2-aminoethoxy)ethoxy)ethyl)amino)butoxy)phenyl)-N-(2-(benzylamino)-1-(4-bromophenyl)-2-oxoethyl)-N-cyclopropylpropanamide (**23**): **18** (600 mg, 0.93 mmol), K_2CO_3 (250 mg, 1.80 mmol) and 2,2´-(ethylenedioxy)bis(ethylamine) (675 µL, 4.59 mmol) were suspended in absolute CH_3CN (10 mL) under Argon atmosphere. The reaction mixture refluxed 4 h at 100 °C. Afterwards the suspension was filtered, the filtrate concentrated *in vacuo* and the crude product purified by MPLC (EtOAc/EtOH/NEt_3 1/1/0.1) to isolate **23** as

yellowish oil (465 mg, 71%). ^{1}H NMR ($CDCl_3$, 400 MHz): δ 7.42-7.38 (m, 2H), 7.32-7.21 (m, 5H), 7.13-7.08 (m, 4H), 6.79-6.77 (m, 2H), 6.45 (t, *J*=5.6 Hz, 1H, NH), 5.53 (s, 1H), 4.49-4.37 (m, 2H), 3.94 (t, *J*=6.4 Hz, 2H), 3.61-3.59 (m, 6H), 3.50 (t, *J*=5.2 Hz, 2H), 2.93-2.84 (m, 6H), 2.81 (t, *J*=5.2 Hz, 2H), 2.69 (t, *J*=7.2 Hz, 2H), 2.49-2.43 (m, 1H), 1.85-1.78 (m, 2H), 1.71-1.64 (m, 2H), 0.93-0.76 (m, 2H), 0.69-0.58 (m, 2H); ^{13}C NMR ($CDCl_3$, 100 MHz): δ 176.4, 169.7, 157.6, 138.1, 134.8, 133.1, 131.7, 130.8, 129.5, 128.7, 127.6, 127.5, 122.1, 114.6, 73.4, 70.6, 70.4, 70.3, 67.8, 66.0, 49.6, 49.3, 43.8, 41.8, 36.5, 31.3, 30.4, 27.2, 26.7, 10.7, 9.3; IR $\tilde{\nu}$ 3312, 2863, 1647, 1509, 1395, 1239, 1106, 1010, 824, 699, 550 cm^{-1}; ESI-MS: *m/2z* 355.6 [M+2H^{+}].

N-(2-(2-(2-((4-(4-(3-((2-(benzylamino)-1-(4-bromophenyl)-2-oxoethyl)(cyclopropyl)amino)-3-oxopropyl)phenoxy)butyl)amino)ethoxy)ethoxy)ethyl)-5-((3aS,4S,6aR)-2-oxohexahydro-1H-thieno[3,4-d]imidazol-4-yl)pentanamide (**24**): NHS-Biotin (81.0 mg, 0.23 mmol) was dissolved in absolute DMF (1.5 mL) under Argon atmosphere. Solution of **23** (200 mg, 0.28 mmol) and DIPEA (100 µL, 0.58 mmol) in absolute DMF (1.5 mL) was added dropwise and the reaction mixture stirred 22 h at r.t. After the solvent was removed *in vacuo* the crude product was directly purified by reversed phase MPLC (H_2O/ CH_3OH 8/2 to 1/9) to isolate **24** as hygroscopic colourless solid (149 mg, 53%). ^{1}H NMR ($CDCl_3$, 400 MHz): δ 7.41-7.39 (m, 2H), 7.32-7.22 (m, 5H), 7.13-7.08 (m, 4H), 6.82-6.77 (m, 3H, NH), 6.63 (dt, *J*=5.8, 17.7 Hz, 1H, NH), 6.27 (d, *J*=8.8 Hz, 1H, NH), 5.58 (s, 1H), 5.38 (d, *J*=7.7 Hz, 1H, NH), 4.94-4.37 (m, 3H), 4.26-4.23 (m, 1H), 3.94 (t, *J*=6.3 Hz, 2H), 3.60-3.58 (m, 6H), 3.54 (t, *J*=4.9 Hz, 2H), 3.43-3.38 (m, 2H), 3.12-3.08 (m, 1H), 2.93-2.79 (m, 8H), 2.71-2.66 (m, 3H), 2.46-2.41 (m, 1H), 2.23-2.16 (m, 2H), 1.85-1.78 (m, 2H), 1.74-1.60 (m, 6H), 1.45-1.37 (m, 2H), 0.94-0.85 (m, 1H), 0.83-0.76 (m, 1H), 0.70-0.57 (m, 2H); ^{13}C NMR ($CDCl_3$, 100 MHz): δ 176.4, 173.3, 169.8, 163.8, 157.5, 138.2, 134.9, 133.2,

131.7, 130.9, 129.5, 128.7, 127.7, 127.4, 122.1, 114.6, 70.5, 70.2 (2C), 70.1, 67.8, 65.8, 61.9, 60.2, 55.6, 49.6, 49.2, 43.8, 40.6, 39.2, 36.4, 36.0, 31.1, 30.4, 28.3, 28.2, 27.2, 26.7, 25.6, 10.7, 9.3; IR $\tilde{\nu}$ 3295, 2923, 1696, 1644, 1509, 1239, 1073, 1010, 567 cm^{-1}; ESI-MS: *m/z* 937.5 $[M+H^+]$.

Cell culture

The human MM cell line INA-6 was a gift from Dr. Martin Gramatzki (Kiel, Germany). Cells were cultured at 37 °C and 5% CO_2, in RPMI medium supplemented with 2 ng/ml interleukin-6, 10% FBS, 100 U/ml penicillin, 100 µg/ml streptomycin, 1 mM sodium pyruvate, 2 mM glutamine (Invitrogen, Darmstadt, Germany).

Assessment of HSR

As described recently,[16] the isolated α-acyl aminocarboxamide compounds were evaluated using an HSP90 inhibitor-based HSR model assay to analyze their ability to inhibit the HSF1-mediated upregulation of multiple HSPs (e.g. HSP72). In brief, INA-6 MM cells were pre-treated either with DMSO as a solvent control or with the compounds **10a-m**, **11a-g** or **18-24** (dissolved in DMSO at a concentration of 50 µM, of note, exceptions were made with substances **23** (12.5 µM) and **19** (25 µM) due to their cytotoxicity at higher concentrations), respectively, for 4 h prior to incubation either with DMSO as a solvent control or with the pharmacological HSP90 inhibitor **25** (resolved in DMSO) as a specific HSF1 inductor for further 4 h. INA-6 cell pellets were dissolved in lysis buffer (20 mM HEPES, pH 7.9), 350 mM NaCl, 1 mM $MgCl_2$, 0.5 mM EDTA, 0.1 mM EGTA, 1% NP40, 0.5 mM dithiothreiol (DTT), 1 mM Na_3VO_4, 0.1 mM PMSF and 1 µg/ml aprotinin. Lysates were cleared by centrifugation, measured by quantitative protein assay (Bio-Rad, München, Germany) and subjected to two complementary readout assays for HSP detection: Western blot for analysis as

a semi-qualitative method (Figure 2) and ELISA for analysis of quantitative HSP72 protein expression (Figure 3). Western blot analyses of HSP72 in INA-6 cells were performed essentially as described before.[13,16,51] In brief, equal quantities of protein lysates were mixed 1:1 with Laemmli buffer and separated by SDS/10%-polyacrylamide gel electrophoresis. Proteins were transferred onto nitrocellulose membranes (Schleicher & Schuell, Dassel, Germany), incubated with antibodies specific for primary antibodies against HSP72 (SPA-810 from Stressgen Bioreagents, Ann Arbor, USA)), HSP27 (ADI-SPA800 from Enzo Life Sciences, Lörrach,Germany), HSF1 or phospho(Ser326)-HSF1 (SPA-905 or SPA902, Stressgen Bioreagents), β-actin as a loading control (A5316, Sigma, Deisenhofen, Germany), α-tubulin (MCA78G, AbD Serotec part of Bio-Rad, Munich, Germany) and Histone H2A.X (Cell Signaling, 7631, Frankfurt am Main, Germany) according to standard procedures and visualized with secondary horseradish peroxidase (HRP)-conjugated antibodies using an enhanced chemoluminescence detection system (ECL, Amersham, Freiburg, Germany). The HSP72-ELISA was performed according to the manufactures instructions (ADI-EKS-700B, Enzo Life Sciences). In brief, recombinant HSP72 protein samples with defined concentrations (in triplicates) or equalized INA-6 whole cell protein lysates (in triplicates) from the above-described two independent approaches were plated on wells and incubated with a rabbit polyclonal anti-Hsp72 antibody prior to further incubation with a horseradish peroxidase conjugated anti-rabbit antibody. Colorimetric reaction was initiated by adding tetramethylbenzidine and measured at 450 nm using a microplate reader (BioRad). Finally, the HSP72 standard curve was plotted and the concentrations of the HSP72 samples were calculated using the Microplate Manager Software from BioRad. Graphs were drawn using GraphPad Prism version 7 (GraphPad software Inc., La Jolla, USA).

Viability assessment

Both apoptotic and viable cell fractions were determined by staining with annexin V-FITC and propidium iodide (PI) according to the manufacturers' instructions (Bender MedSystems, Vienna, Austria). In brief, INA-6 cells were washed with PBS buffer, incubated in binding buffer (10 mM HEPES/NaOH, pH 7.4, 140 mM NaCl, 2.5 mM $CaCl_2$) containing 2.5 mL annexin V-FITC and 1 mg/mL PI, and analyzed by flow cytometry (FACSCalibur/CELLQuest; Becton Dickinson, Heidelberg, Germany). Whereas the early apoptotic stage can only be detected by binding of annexin V to translocated phosphatidylserine residues at the external cell membrane, later apoptotic stages, in which cellular membrane integrity is lost, can additionally visualized by incorporation of the DNA-binding agent PI. Thus, the cell fraction that is negative for both annexin V-FITC and PI is considered viable. Based on the respective INA-6 viable cell fractions the means, standard deviations, dose-response curves and EC_{50} values for the compounds **19** and **23** were calculated using the GraphPad Prism software version 7. The effects of the compounds **19**, **23** or **10d** on MM tumor cell survival was analyzed in the MM cell line model INA-6. INA-6 cells were either incubated with DMSO as a solvent control or with increasing concentrations of **19**, **23** or **10d** for 72 h prior to harvesting and viability assessment. For combination experiments, INA-6 cells were incubated with sub-maximally effective concentrations either of the compound **19** (7 µM; for 72 h), the HSP90 inhibitor **25** (10 nM; for 68 h), or a combination of both compounds. 4 h after the treatment start with either with DMSO as a solvent control or compound **19**, either DMSO or 10 nM of **25** were added for an additional 68 h followed by flow cytometry-based viability analysis.

Real-time PCR

Total RNA was isolated from 1x10^6 cells using the PEQGold total RNA Kit (S-Line) (PEQLab, VWR, Erlangen, Germany) according to the manufacturers' guidelines. First-strand cDNA synthesis as done by using the High Capacity cDNA Reverse Transcription Kit with RNase Inhibitor (Applied Biosystems, Darmstadt, Germany) and random hexamer primers according to manufacturer's protocol.

Gene-specific primers for real-time PCR were designed using Primer Express 3.0 (Applied Biosystems) and primer-target specificity was checked using nucleotide BLAST program (http://blast.ncbi.nlm.nih.gov). For real-time PCR, Luna Universal qPCR master mix (New England Biolabs, Frankfurt am Main, Germany) was used according to the manufacturer's instructions. PCR was performed in duplicates on a StepOne Plus qPCR instrument (Thermo Fisher Scientific, Darmstadt, Germany) with the following cycling program: 1 min denaturation at 95°C, followed by 40 cycles of 95°C for 15 s and 60°C for 30 s. A final denaturation-annealing step was performed at 95°C for 15 s and 1 min at 60°C. Thereafter, PCR products were analysed by thermal dissociation curve and by agarose gel electrophoresis to verify specific PCR product amplification. Data were normalized against the reference gene α-tubulin. The primer sequences of the genes used in this study are the following: α-tubulin_fwd: CCACATATGCCCCTGTCATCT, α-tubulin_rev: CATGGCGAGGGTCACATTTC; HSP27_fwd: TCCCTGGATGTCAACCACTTC, HSP27_rev: GCGTGTATTTCCGCGTGAA; HSP72_fwd: AACCAGGTGGCGCTGAAC, HSP72_rev: GGCTTGTCTCCGTCGTTGAT; HSF1_fwd: CCAGCAACAGAAAGTCGTCAAC, HSF1_rev: ATGTGCTGAGCCACTGTCGTT.

Experiment with the DNA-PK inhibitor 26

INA-6 MM cells were pre-treated either with DMSO as a solvent control or with the DNA-PK inhibitor **26** (Tocris, dissolved in DMSO at a concertation of 10 µM), respectively, for 4 h prior to incubation either with DMSO as a solvent control or with the pharmacological HSP90 inhibitor **25** (resolved in DMSO) as a specific HSF1 inductor for further 4 h. Afterwards, cells were pelleted and RNA and protein were extracted and the respective genes / proteins were analysed by real-time PCR and Western blot.

Drug Target Identification: *Magnetic bead preparation:*

Pierce streptavidin magnetic beads (cat. no. 88816, Thermo) and biotinylated inhibitor in DMSO were equilibrated to room temperature. For each sample, 50 µL bead slurry were washed with 500 µL of a 1:1 mixture of DMSO and 50 mM borate buffer pH 8.5. To saturate the beads with inhibitor we used 500 nmol of the biotinylated inhibitor in 400 µL of a 1:1 mixture of DMSO and 50 mM borate buffer pH 8.5. Streptavidin beads and biotinylated inhibitor were incubated (under rotation) overnight at room temperature. Control beads were prepared without inhibitor accordingly. The supernatant was discarded and the beads were washed twice with 1 mL of 50% DMSO. After a second wash, bead slurry was transferred to a new reaction tube and was washed again twice with 500 µL Pierce IP lysis buffer (cat. no. 87787, Thermo).

Cell lysis: INA-6 cells ($5x10^7$) were lysed with 2 mL IP Pierce lysis buffer together with 20 µL Halt protease inhibitor cocktail (cat. no. 78430, Thermo). Cells were incubated on ice for 10 min with periodic mixing. Lysates were cleared by centrifugation at 16.000 x g at 4 °C for 5 min, and protein concentration was determined (BCA Protein Assay, Thermo).

Drug target enrichment: Inhibitor-loaded beads and control beads were incubated with cleared INA-6 cell lysate (5 mg total protein) for 3 h at 4 °C and overhead rotation. Beads were washed four times with 1 mL 20 mM HEPES buffer pH 7.5, 115 mM NaCl, 1.2 mM $CaCl_2$, 1.2 mM $MgCl_2$, 2.4 mM K_2HPO_4, 0.5% NP-40. Proteins were eluted with 360 µL 1 x LDS sample buffer (Invitrogen) and reduced by adding 40 µL 500 mM DTT and boiling the sample for 10 min at 70 °C. Samples were alkylated with final concentration of 120 mM iodoacetamide at room temperature in the dark. The eluates were separated from the beads with a magnet. Proteins were precipitated by adding the fourfold sample volume of acetone. Precipitation was performed overnight at -20 °C. Pellets were washed three times with 1 mL acetone.

In-solution digestion: Precipitated proteins were dissolved in 0.5% sodium deoxycholate (SDC, Sigma-Aldrich) in 100 mM ammonium hydrogencarbonate. Digests were performed with trypsin (trypsin-to-protein ratio: 1:200) overnight at 37 °C. SDC was removed by extraction with ethylacetate.[52] Peptides were dried in a vacuum concentrator (Concentrator 5301, Eppendorf) to remove remaining ethylaceate. Peptides were desalted using C18 stage tips.[53] Each Stage Tip was prepared with three disks of C18 Empore SPE disks (3M) in a 200 µL pipet tip. Peptides were eluted with 80% acetonitrile / 0.1% formic acid, dried in a vacuum concentrator, and stored at -20 °C. Peptides were dissolved in 2% acetonitrile / 0.1% formic acid prior to nanoLC-MS/MS analysis.

Gel electrophoresis: Samples were solved in 1 x LDS sample buffer (Invitrogen) and separated on NuPAGE Novex 4-12% Bis-Tris gels (Invitrogen) with MOPS buffer according to manufacturer's instructions. Gels were washed three times for 5 min with water and stained for 45 min with Simply Blue Safe Stain (Invitrogen). After washing with water for 1 hour, each lane was cut into 15 bands.

In-gel digestion: The excised gel bands were destained with 30% acetonitrile in 0.1 M NH_4HCO_3 (pH 8), shrunk with 100% acetonitrile, and dried in a vacuum concentrator (Concentrator 5301, Eppendorf). Digests were performed with 0.1 µg trypsin per gel band overnight at 37 °C in 0.1 M NH_4HCO_3 (pH 8). After removing the supernatant, peptides were extracted from the gel slices with 5% formic acid, and extracted peptides were pooled with the supernatant.

NanoLC-MS/MS analysis: NanoLC-MS/MS analyses were performed on an Orbitrap Fusion or an Orbitrap Velos Pro (Thermo) equipped with EASY-Spray ion source and coupled to an EASY-nLC 1000 (Thermo). Peptides were loaded on a trapping column (2 cm x 75 µm ID, PepMap C18, 3 µm particles, 100 Å pore size) and separated on EASY-Spray analytical columns (75 µm ID, PepMap C18, 2 µm particles, 100 Å pore size reverse phase material) with 200 nL/min flow and linear gradients from 3% to 32% acetonitrile / 0.1% formic acid.

In-solution digests were analyzed with 50 cm analytical columns and a 180-min gradient on the Fusion instrument (MS scan resolution of 60,000, MS/MS scan resolution 7,500, HCD fragmentation, top speed method with max. 3 sec cycle time).

In-gel digests were analyzed with 25 cm columns and 30-min gradients either on the Orbitrap Fusion (otherwise same method as above) or the Orbitrap Velos instrument with a MS scan resolution of 30,000. Velos MS/MS scans were acquired either in the Orbitrap (resolution 7,500, HCD fragmentation, top 5 method) or in the ion trap (CID fragmentation, top 15 method).

Singly charged precursors were excluded from selection and a dynamic exclusion list was applied. EASY-IC (Fusion) or lock-mass (Velos) was used for internal calibration for all runs.

MS data analysis: For MS raw data file processing, database searches and quantification, MaxQuant version 1.5.3.30 was used.[54] Searches were performed against the *H. sapiens* reference proteome database (UniProt) and additionally, a database containing common contaminants. The search was performed with tryptic cleavage specificity with three allowed miscleavages.

Protein identification was under control of the false-discovery rate (< 1% FDR on protein and peptide level). In addition to MaxQuant default settings, the search was performed against following variable modifications: Protein N-terminal acetylation, Gln to pyro-Glu formation (N-term. Gln) and oxidation (Met). For protein quantification, LFQ intensities were used.[55] Protein groups with less than two identified razor/unique peptides were dismissed. Experiments for which in-solution and in-gel digests were performed, were combined as technical replicates during analysis.

For further data analysis, in-house developed R scripts were used. Missing LFQ intensities in the control samples were imputed with values close to the baseline, i.e. with values from a standard normal distribution with a mean of the 1% quantile of the log10-transformed LFQ intensities (of inhibitor and corresponding control sample) and a standard deviation of 0.05. For the identification of significantly enriched proteins within the replicate experiments, the R package limma was used[56] and proteins were considered enriched significantly with ratios in at least two biological replicates and a Benjamini-Hochberg adjusted p-value of 0.02 or lower, which corresponds to a q-value of 2% (FDR). For comparison between different affinity capture experiments, log2 protein ratios were standardized (Z-score). Here, all median log2 protein ratios inhibitor/control (with n replicates > 1) were devided by the

standard deviation of all median log2 ratios. For data plotting, missing z-scores were replaced by “0”.

For Interpro-domain[57] enrichment analysis, Fisher´s exact test was applied with significantly enriched proteins (q < 0.02 and n>1 and median log2 protein ratio > 0) and unspecific binders (q >= 0.02 and n>1).

Associated content

Supplemental Information: Detailed synthesis procedures of compounds **10a-m** and **11a-g**, structure characterization and NMR spectra from selected substances are available in Supplemental Information. Furthermore, detailed results from affinity capture experiments are listed in the Supplemental Information. This material is available free of charge via the Internet at http://pubs.acs.org

AUTHOR INFORMATION

Corresponding Authors:

*Prof. Dr. Ulrike Holzgrabe, E-mail: ulrike.holzgrabe@uni-wuerzburg.de, Tel.: 0049-931- 3185460;

*Prof. Dr. Andreas Schlosser, E-mail: andreas.schlosser@virchow.uni-wuerzburg.de, Tel.: 0049-931-3186888;

*Dr. Manik Chatterjee, E-mail: chatterjee_m@ukw.de, Tel.: 0049-931-201-36414.

Notes

The authors declare no competing financial interests.

Author Contributions

The manuscript was written through contributions of all authors. All authors have given approval to the final version of the manuscript. M.B., A.L. and D.B. contributed equally. U.H., A.S. and M.C. conceived the project. A.H. designed and synthesised the compounds **10a**-**m** and **11a,b**. A.L. designed and synthesised the compounds **11c-g** and **17-24**. All compounds were biologically evaluated by D.B. M.B. performed the affinity capture experiments and analysed MS data. J.T.V statistically analysed quantitative MS data and performed bioinformatics.

ACKNOWLEDGEMENT

We gratefully acknowledge the financial support by the Deutsche Forschungsgemeinschaft given to U.H., A.S. and M.C. (CRU216). We thank Heike Schraud and Stefanie Kressmann for excellent technical assistance.

ABBREVIATIONS

DIPEA, *N*,*N*-Diisopropylethylamine; DMF, Dimethylformamide; HPLC, high-performance liquid chromatography; LFQ, label free quantification; MS, mass spectrometry; MM, multiple myeloma; MPLC, Medium pressure liquid chromatography; NMR, nuclear magnetic resonance; PAINS, pan-assay interference compounds; TLC, thin layer chromatography; U-4CR, Ugi 4-component reaction.

References

1. Lindquist, S. The heat-shock response. *Annu. Rev. Biochem.* **1986,** *55*, 1151-1191.

2. Georgopoulos, C.; Welch, W. J. Role of the major heat shock proteins as molecular chaperones. *Annu. Rev. Cell Biol.* **1993,** *9*, 601-634.

3. Calderwood, S. K. HSF1, a versatile factor in tumorogenesis. *Curr. Mol. Med.* **2012,** *12* (9), 1102-1107.

4. Ciocca, D. R.; Arrigo, A. P.; Calderwood, S. K. Heat shock proteins and heat shock factor 1 in carcinogenesis and tumor development: an update. *Arch. Toxicol.* **2013,** *87* (1), 19-48.

5. Calderwood, S. K.; Khaleque, M. A.; Sawyer, D. B.; Ciocca, D. R. Heat shock proteins in cancer: chaperones of tumorigenesis. *Trends Biochem. Sci.* **2006,** *31* (3), 164-172.

6. Ciocca, D. R.; Calderwood, S. K. Heat shock proteins in cancer: diagnostic, prognostic, predictive, and treatment implications. *Cell Stress Chaperones* **2005,** *10* (2), 86-103.

7. Evans, C. G.; Chang, L.; Gestwicki, J. E. Heat shock protein 70 (hsp70) as an emerging drug target. *J. Med. Chem.* **2010,** *53* (12), 4585-4602.

8. Calderwood, S. K.; Neckers, L. Hsp90 in cancer: transcriptional roles in the nucleus. *Adv. Cancer Res.* **2016,** *129*, 89-106.

9. Gerecke, C.; Fuhrmann, S.; Strifler, S.; Schmidt-Hieber, M.; Einsele, H.; Knop, S. The diagnosis and treatment of multiple myeloma. *Dtsch. Arztebl. Int.* **2016,** *113* (27-28), 470-476.

10. Sonneveld, P.; Broijl, A. Treatment of relapsed and refractory multiple myeloma. *Haematologica* **2016,** *101* (8), 995.

11. Mitsiades, C. S.; Mitsiades, N. S.; McMullan, C. J.; Poulaki, V.; Kung, A. L.; Davies, F. E.; Morgan, G.; Akiyama, M.; Shringarpure, R.; Munshi, N. C.; Richardson, P. G.; Hideshima, T.; Chauhan, D.; Gu, X.; Bailey, C.; Joseph, M.; Libermann, T. A.; Rosen, N. S.; Anderson, K. C. Antimyeloma activity of heat shock protein-90 inhibition. *Blood* **2006,** *107* (3), 1092-1100.

12. Chatterjee, M.; Jain, S.; Stühmer, T.; Andrulis, M.; Ungethum, U.; Kuban, R. J.; Lorentz, H.; Bommert, K.; Topp, M.; Kramer, D.; Müller-Hermelink, H. K.; Einsele, H.; Greiner, A.; Bargou, R. C. STAT3 and MAPK signaling maintain overexpression of heat shock proteins 90alpha and beta in multiple myeloma cells, which critically contribute to tumor-cell survival. *Blood* **2007,** *109* (2), 720-728.

13. Chatterjee, M.; Andrulis, M.; Stühmer, T.; Müller, E.; Hofmann, C.; Steinbrunn, T.; Heimberger, T.; Schraud, H.; Kressmann, S.; Einsele, H.; Bargou, R. C. The PI3K/Akt signaling pathway regulates the expression of Hsp70, which critically contributes to Hsp90-chaperone function and tumor cell survival in multiple myeloma. *Haematologica* **2013,** *98* (7), 1132-1141.

14. Rasche, L.; Duell, J.; Morgner, C.; Chatterjee, M.; Hensel, F.; Rosenwald, A.; Einsele, H.; Topp, M. S.; Brändlein, S. The natural human IgM antibody PAT-SM6 induces apoptosis in primary human multiple myeloma cells by targeting heat shock protein GRP78. *PLoS One* **2013,** *8* (5), e63414.

15. Zhang, L.; Fok, J. H.; Davies, F. E. Heat shock proteins in multiple myeloma. *Oncotarget* **2014,** *5* (5), 1132-1148.

16. Heimberger, T.; Andrulis, M.; Riedel, S.; Stühmer, T.; Schraud, H.; Beilhack, A.; Bumm, T.; Bogen, B.; Einsele, H.; Bargou, R. C.; Chatterjee, M. The heat shock transcription factor 1 as a potential new therapeutic target in multiple myeloma. *Br. J. Haematol.* **2013,** *160* (4), 465-476.

17. De Thonel, A.; Mezger, V.; Garrido, C. Implication of heat shock factors in tumorigenesis: therapeutical potential. *Cancers (Basel)* **2011,** *3* (1), 1158-1181.

18. Whitesell, L.; Lindquist, S. Inhibiting the transcription factor HSF1 as an anticancer strategy. *Expert Opin. Ther.Targets* **2009,** *13* (4), 469-478.

19. Rye, C. S.; Chessum, N. E.; Lamont, S.; Pike, K. G.; Faulder, P.; Demeritt, J.; Kemmitt, P.; Tucker, J.; Zani, L.; Cheeseman, M. D.; Isaac, R.; Goodwin, L.; Boros, J.; Raynaud, F.; Hayes, A.; Henley, A. T.; de Billy, E.; Lynch, C. J.; Sharp, S. Y.; Te Poele, R.; Fee, L. O.; Foote, K. M.; Green, S.; Workman, P.; Jones, K. Discovery of 4,6-disubstituted pyrimidines as potent inhibitors of the heat shock factor 1 (HSF1) stress pathway and CDK9. *Medchemcomm.* **2016,** *7* (8), 1580-1586.

20. Cheeseman, M. D.; Chessum, N. E.; Rye, C. S.; Pasqua, A. E.; Tucker, M. J.; Wilding, B.; Evans, L. E.; Lepri, S.; Richards, M.; Sharp, S. Y.; Ali, S.; Rowlands, M.; O'Fee, L.; Miah, A.; Hayes, A.; Henley, A. T.; Powers, M.; Te Poele, R.; De Billy, E.; Pellegrino, L.; Raynaud, F.; Burke, R.; van Montfort, R. L.; Eccles, S. A.; Workman, P.; Jones, K. Discovery of a chemical probe bisamide (CCT251236): an orally bioavailable efficacious pirin ligand from a heat shock transcription factor 1 (HSF1) phenotypic screen. *J. Med. Chem.* **2017,** *60* (1), 180-201.

21. Hosokawa, N.; Hirayoshi, K.; Nakai, A.; Hosokawa, Y.; Marui, N.; Yoshida, M.; Sakai, T.; Nishino, H.; Aoike, A.; et, a. Flavonoids inhibit the expression of heat shock proteins. *Cell Struct. Funct.* **1990,** *15* (6), 393-401.

22. Yokota, S.-I.; Kitahara, M.; Nagata, K. Benzylidene lactam compound, KNK437, a novel inhibitor of acquisition of thermotolerance and heat shock protein induction in human colon carcinoma cells. *Cancer Res.* **2000,** *60* (11), 2942-2948.

23. Akagawa, H.; Takano, Y.; Ishii, A.; Mizuno, S.; Izui, R.; Sameshima, T.; Kawamura, N.; Dobashi, K.; Yoshioka, T. Stresgenin B, an inhibitor of heat-induced heat shock protein gene expression, produced by Streptomyces sp. AS-9. *J. Antibiot.* **1999,** *52* (11), 960-970.

24. Westerheide, S. D.; Kawahara, T. L.; Orton, K.; Morimoto, R. I. Triptolide, an inhibitor of the human heat shock response that enhances stress-induced cell death. *J. Biol. Chem.* **2006,** *281* (14), 9616-9622.

25. Santagata, S.; Xu, Y. M.; Wijeratne, E. M.; Kontnik, R.; Rooney, C.; Perley, C. C.; Kwon, H.; Clardy, J.; Kesari, S.; Whitesell, L.; Lindquist, S.; Gunatilaka, A. A. Using the heat-shock response to discover anticancer compounds that target protein homeostasis. *ACS Chem. Biol.* **2012,** *7* (2), 340-349.

26. Domling, A.; Ugi, I. I. Multicomponent reactions with isocyanides. *Angew. Chem. Int. Ed. Engl.* **2000,** *39* (18), 3168-3210.

27. Baell, J. B.; Holloway, G. A. New substructure filters for removal of pan assay interference compounds (PAINS) from screening libraries and for their exclusion in bioassays. *J. Med. Chem.* **2010,** *53* (7), 2719-2740.

28. Baell, J.; Walters, M. A. Chemistry: Chemical con artists foil drug discovery. *Nature* **2014,** *513* (7519), 481-483.

29. EU, Committee for Medicinal Products for Human Use (CHMP) - Giotrif - EMA/491185/2013, Procedure No. EMEA/H/C/002280. 2013.

30. Burger, J. A.; Tedeschi, A.; Barr, P. M.; Robak, T.; Owen, C.; Ghia, P.; Bairey, O.; Hillmen, P.; Bartlett, N. L.; Li, J.; Simpson, D.; Grosicki, S.; Devereux, S.; McCarthy, H.; Coutre, S.; Quach, H.; Gaidano, G.; Maslyak, Z.; Stevens, D. A.; Janssens, A.; Offner, F.; Mayer, J.; O'Dwyer, M.; Hellmann, A.; Schuh, A.; Siddiqi, T.; Polliack, A.; Tam, C. S.; Suri, D.; Cheng, M.; Clow, F.; Styles, L.; James, D.

F.; Kipps, T. J.; Investigators, R.-. Ibrutinib as initial therapy for patients with chronic lymphocytic leukemia. *N. Engl. J. Med.* **2015,** *373* (25), 2425-2437.

31. I. Ugi, C. S. Über ein neues Kondensations-Prinzip. *Angew. Chem.* **1960,** *72*, 267-268.

32. Hartung, A.; Seufert, F.; Berges, C.; Gessner, V.; Holzgrabe, U. One-Pot Ugi/Aza-Michael Synthesis of Highly Substituted 2,5-Diketopiperazines with Anti-Proliferative Properties. *Molecules* **2012,** *17* (12), 14685-14699.

33. Meanwell, N. A. Improving drug candidates by design: a focus on physicochemical properties as a means of improving compound disposition and safety. *Chem. Res. Toxicol.* **2011,** *24* (9), 1420-1456.

34. Jiang, W.; Nowosinski, K.; Low, N. L.; Dzyuba, E. V.; Klautzsch, F.; Schafer, A.; Huuskonen, J.; Rissanen, K.; Schalley, C. A. Chelate cooperativity and spacer length effects on the assembly thermodynamics and kinetics of divalent pseudorotaxanes. *J. Am. Chem. Soc.* **2012,** *134* (3), 1860-1868.

35. Brough, P. A.; Aherne, W.; Barril, X.; Borgognoni, J.; Boxall, K.; Cansfield, J. E.; Cheung, K. M.; Collins, I.; Davies, N. G.; Drysdale, M. J.; Dymock, B.; Eccles, S. A.; Finch, H.; Fink, A.; Hayes, A.; Howes, R.; Hubbard, R. E.; James, K.; Jordan, A. M.; Lockie, A.; Martins, V.; Massey, A.; Matthews, T. P.; McDonald, E.; Northfield, C. J.; Pearl, L. H.; Prodromou, C.; Ray, S.; Raynaud, F. I.; Roughley, S. D.; Sharp, S. Y.; Surgenor, A.; Walmsley, D. L.; Webb, P.; Wood, M.; Workman, P.; Wright, L. 4,5-diarylisoxazole Hsp90 chaperone inhibitors: potential therapeutic agents for the treatment of cancer. *J. Med. Chem.* **2008,** *51* (2), 196-218.

36. Xie, J.; Marusich, M. F.; Souda, P.; Whitelegge, J.; Capaldi, R. A. The mitochondrial inner membrane protein mitofilin exists as a complex with SAM50, metaxins 1 and 2, coiled-coil-helix coiled-coil-helix domain-containing protein 3 and 6 and DnaJC11. *FEBS Lett.* **2007,** *581* (18), 3545-3549.

37. Gubitz, A. K.; Feng, W.; Dreyfuss, G. The SMN complex. *Exp. Cell Res.* **2004,** *296* (1), 51-56.

38. Collart, M. A.; Panasenko, O. O. The CCR4--not complex. *Gene* **2012,** *492* (1), 42-53.

39. Rusin, S. F.; Schlosser, K. A.; Adamo, M. E.; Kettenbach, A. N. Quantitative phosphoproteomics reveals new roles for the protein phosphatase PP6 in mitotic cells. *Sci. Signal.* **2015,** *8* (398), rs12.

40. Weber, A. M.; Ryan, A. J. ATM and ATR as therapeutic targets in cancer. *Pharmacol. Ther.* **2015,** *149*, 124-138.

41. Tu, Y.; Ji, C.; Yang, B.; Yang, Z.; Gu, H.; Lu, C. C.; Wang, R.; Su, Z. L.; Chen, B.; Sun, W. L.; Xia, J. P.; Bi, Z. G.; He, L. DNA-dependent protein kinase catalytic subunit (DNA-PKcs)-SIN1 association mediates ultraviolet B (UVB)-induced Akt Ser-473 phosphorylation and skin cell survival. *Mol. Cancer* **2013,** *12* (1), 172.

42. Sarbassov, D. D.; Ali, S. M.; Sabatini, D. M. Growing roles for the mTOR pathway. *Curr. Opin. Cell Biol.* **2005,** *17* (6), 596-603.

43. Huang, J.; Nueda, A.; Yoo, S.; Dynan, W. S. Heat shock transcription factor 1 binds selectively in vitro to Ku protein and the catalytic subunit of the DNA-dependent protein kinase. *J. Biol. Chem.* **1997,** *272* (41), 26009-26016.

44. Nueda, A.; Hudson, F.; Mivechi, N. F.; Dynan, W. S. DNA-dependent protein kinase protects against heat-induced apoptosis. *J. Biol. Chem.* **1999,** *274* (21), 14988-14996.

45. Baretic, D.; Williams, R. L. PIKKs--the solenoid nest where partners and kinases meet. *Curr. Opin. Struct. Biol.* **2014,** *29*, 134-142.

46. Lopez, Y.; Nakai, K.; Patil, A. HitPredict version 4: comprehensive reliability scoring of physical protein-protein interactions from more than 100 species. *Database* **2015,** *2015*, 1-10.

47. Dahlstrom, K. M.; Salminen, T. A. 3D model for cancerous inhibitor of protein phosphatase 2A armadillo domain unveils highly conserved protein-protein interaction characteristics. *J. Theor. Biol.* **2015,** *386*, 78-88.

48. Leahy, J. J.; Golding, B. T.; Griffin, R. J.; Hardcastle, I. R.; Richardson, C.; Rigoreau, L.; Smith, G. C. Identification of a highly potent and selective DNA-dependent protein kinase (DNA-PK) inhibitor (NU7441) by screening of chromenone libraries. *Bioorg. Med. Chem. Lett.* **2004,** *14* (24), 6083-6087.

49. Jaeger, A. M.; Makley, L. N.; Gestwicki, J. E.; Thiele, D. J. Genomic heat shock element sequences drive cooperative human heat shock factor 1 DNA binding and selectivity. *J. Biol. Chem.* **2014,** *289* (44), 30459-30469.

50. Gottlieb, H. E.; Kotlyar, V.; Nudelman, A. NMR chemical shifts of common laboratory solvents as trace impurities. *J. Org. Chem.* **1997,** *62* (21), 7512-7515.

51. Chatterjee, M.; Honemann, D.; Lentzsch, S.; Bommert, K.; Sers, C.; Herrmann, P.; Mathas, S.; Dorken, B.; Bargou, R. C. In the presence of bone marrow stromal cells human multiple myeloma cells become independent of the IL-6/gp130/STAT3 pathway. *Blood* **2002,** *100* (9), 3311-3318.

52. Masuda, T.; Tomita, M.; Ishihama, Y. Phase transfer surfactant-aided trypsin digestion for membrane proteome analysis. *J. Proteome Res.* **2008,** *7* (2), 731-740.

53. Rappsilber, J.; Ishihama, Y.; Mann, M. Stop and go extraction tips for matrix-assisted laser desorption/ionization, nanoelectrospray, and LC/MS sample pretreatment in proteomics. *Anal. Chem.* **2003,** *75* (3), 663-670.

54. Cox, J.; Mann, M. MaxQuant enables high peptide identification rates, individualized p.p.b.-range mass accuracies and proteome-wide protein quantification. *Nat. Biotechnol.* **2008,** *26* (12), 1367-1372.

55. Cox, J.; Hein, M. Y.; Luber, C. A.; Paron, I.; Nagaraj, N.; Mann, M. Accurate proteome-wide label-free quantification by delayed normalization and maximal peptide ratio extraction, termed MaxLFQ. *Mol. Cell Proteomics* **2014,** *13* (9), 2513-2526.

56. Ritchie, M. E.; Phipson, B.; Wu, D.; Hu, Y.; Law, C. W.; Shi, W.; Smyth, G. K. limma powers differential expression analyses for RNA-sequencing and microarray studies. *Nucleic Acids Res.* **2015,** *43* (7), e47.

57. Mitchell, A.; Chang, H. Y.; Daugherty, L.; Fraser, M.; Hunter, S.; Lopez, R.; McAnulla, C.; McMenamin, C.; Nuka, G.; Pesseat, S.; Sangrador-Vegas, A.; Scheremetjew, M.; Rato, C.; Yong, S. Y.; Bateman, A.; Punta, M.; Attwood, T. K.; Sigrist, C. J.; Redaschi, N.; Rivoire, C.; Xenarios, I.; Kahn, D.; Guyot, D.; Bork, P.; Letunic, I.; Gough, J.; Oates, M.; Haft, D.; Huang, H.; Natale, D. A.; Wu, C. H.; Orengo, C.; Sillitoe, I.; Mi, H.; Thomas, P. D.; Finn, R. D. The InterPro protein families database: the classification resource after 15 years. *Nucleic Acids Res.* **2015,** *43* (Database issue), D213-221.

Table of Content